이학석사학위논문

Analysis of Marine Magnetic Field Anomaly and Multi-beam Bathymetry Profiles of the West Philippine Basin and Its Style of Opening

서필리핀분지의 분지발달과정이해를 위한 해양지자기이상대 및 다중 빔 음향측심 분석

2016년 8월

서울대학교 대학원

지구환경과학부

최 한 진

Analysis of Marine Magnetic Field Anomaly and Multi-beam Bathymetry Profiles of the West Philippine Basin and Its Style of Opening

Hanjin Choe

A dissertation submitted in partial fulfillment
of the requirements for the degree of Master in Natural Science

School of Earth and Environmental Science
Graduate School
Seoul National University

ABSTRACT

The West Philippine Basin (WPB), located on the Philippine Sea Plate, is considered to have undergone a rapid opening during the Eocene. However, the detailed opening of the WPB and its relationship with surrounding basins were rather uncertain in the previous plate reconstruction models because of, for instance, (1) the limited marine magnetic data coverage, (2) highly skewed and weak magnetic anomalies by complex basin formation, (3) impossible to analyze subducted part of the basin. This study re-examines the opening of the WPB with the sea surface marine magnetic anomalies and multi-beam echo sounder data that were added to the database over the last several decades. The shipboard three component magnetometer (STCM) is an efficient instrument not only to obtain data without additional sensor manipulations but also to compare the observed magnetic anomaly with 2-D synthetic model because the vertical component magnetic anomaly is not affected by skewed horizontal magnetic field. However, the STCM data is complicated to remove the noise caused by position of the ship and its induced magnetization. In order to corroborate the validity of the STCM data, therefore, the magnetic boundary strike diagrams (MBSD) were computed to compare with the seafloor fabric trends and magnetic isochrons, which showed good connections. Based on this reliability, the magnetic isochrons could be identified to chron 22y and detailed rotation poles for different stages were computed by Gplates program. The calculated kinematic values indicate that the WPB started opening in

ENE-WSW direction in chron 22y (> 49 Ma) but changed gradually to N-S direction in chron 21y (45 Ma). The time dependent rms spreading speed of this study is faster than that of previous reports. The opening suddenly slowed down in 37 Ma then finally ceased in 26 Ma. According to our analysis, the observed asymmetric spreading between north and south became more pronounced towards the end of the opening. Although marine magnetic anomaly data are too ambiguous to discern if plate is subducted or under complex formation, it provides vital constraints for a reconstructing plate kinematic model.

Keywords: West Philippine Basin, Euler pole, magnetic anomaly, isochron, plate reconstruction

Student Number: 2012-23083

TABLE OF CONTENTS

LIST OF FIGURES

LIST OF TABLES

1. INTRODUCTION

The Philippine Sea Plate (PSP), an oceanic plate consisting of complex tectonic terrains, has been extensively studied ever since Hess (1948) found the existence of the Central Basin Ridge (CBR). The PSP is quite unique because it is almost completely surrounded by subduction zones except for the southernmost part. Furthermore, it is being subducted on the west below Eurasian plate while overriding the Pacific plate on the east (Fig. 1).

The West Philippine Basin (WPB) is the oldest basin in the PSP, occupying the western side, and is considered to be a region where the early development of the PSP can be investigated. A unique characteristic of the WPB is that it exhibits a complicated seafloor topography and crustal structures with notable differences in topography between the east and the west of CBR (Okino et al. 1999). Unlike normal oceanic basins that opened in Eocene whose depth is 4800-5000 m (Crosby et al., 2006), the depth of the WPB is 5800-6000-m-deep seafloor (Mrozowski et al., 1982). Also, the crustal thickness is inconsistent: The thickness of the east basin is thin while that of the west part is similar as the Pacific Plate (Louden, 1980; Goodman and Bibee, 1988; Ishihara et al., 2007). The detailed opening of the WPB and its interaction with surrounding basins are not well understood. Thin oceanic crust and complicated opening process generated skewed and complex magnetic anomaly patterns. For these reasons, the detailed opening of the WPB and its relationship with surrounding basins were rather uncertain in the previous plate reconstruction models.

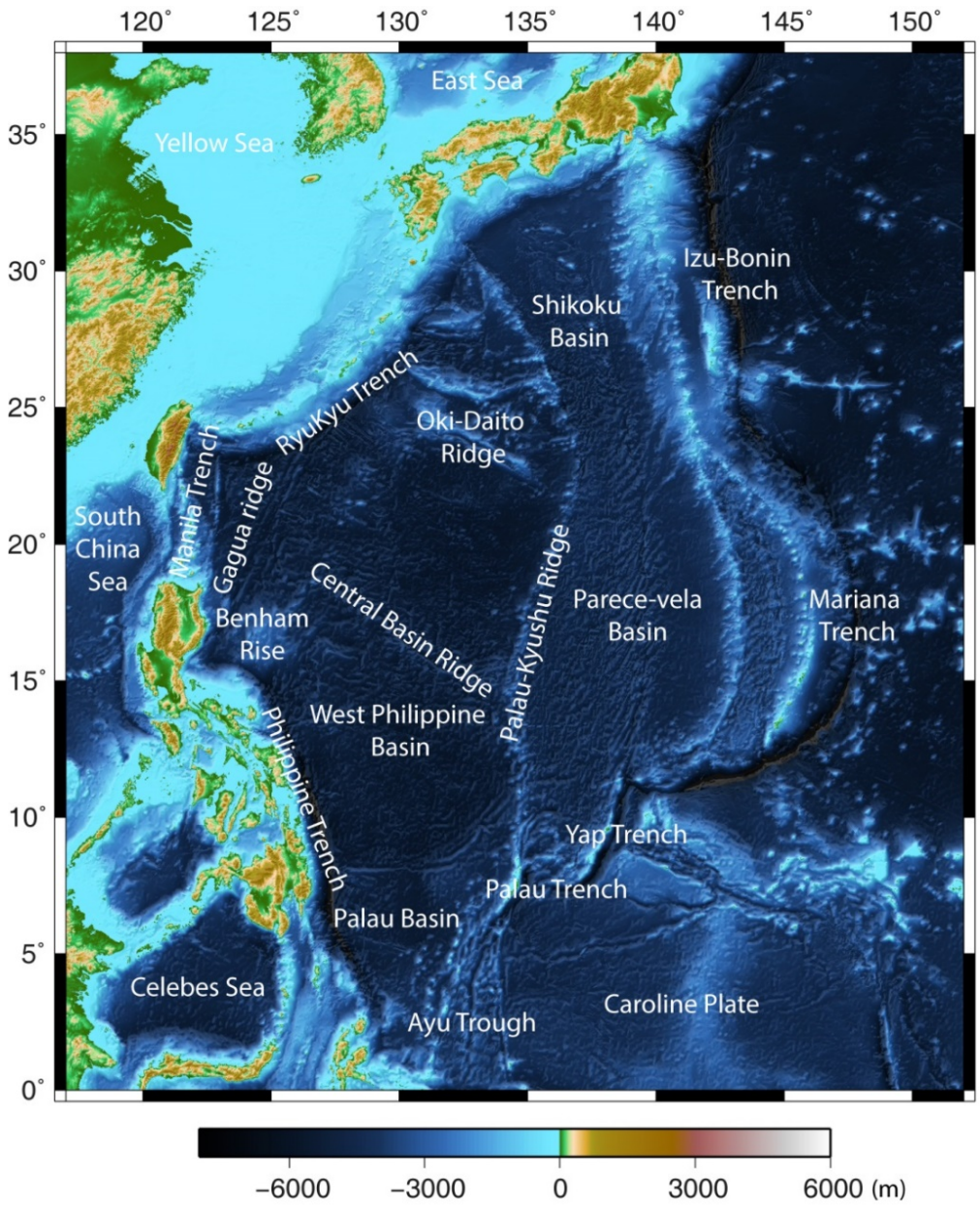

Figure 1 Shaded bathymetry map of the Philippine Sea Plate. The bathymetry grid derived from satellite altimetry, ETOPO1 (Sandwell and Smith 1997), was applied to the background

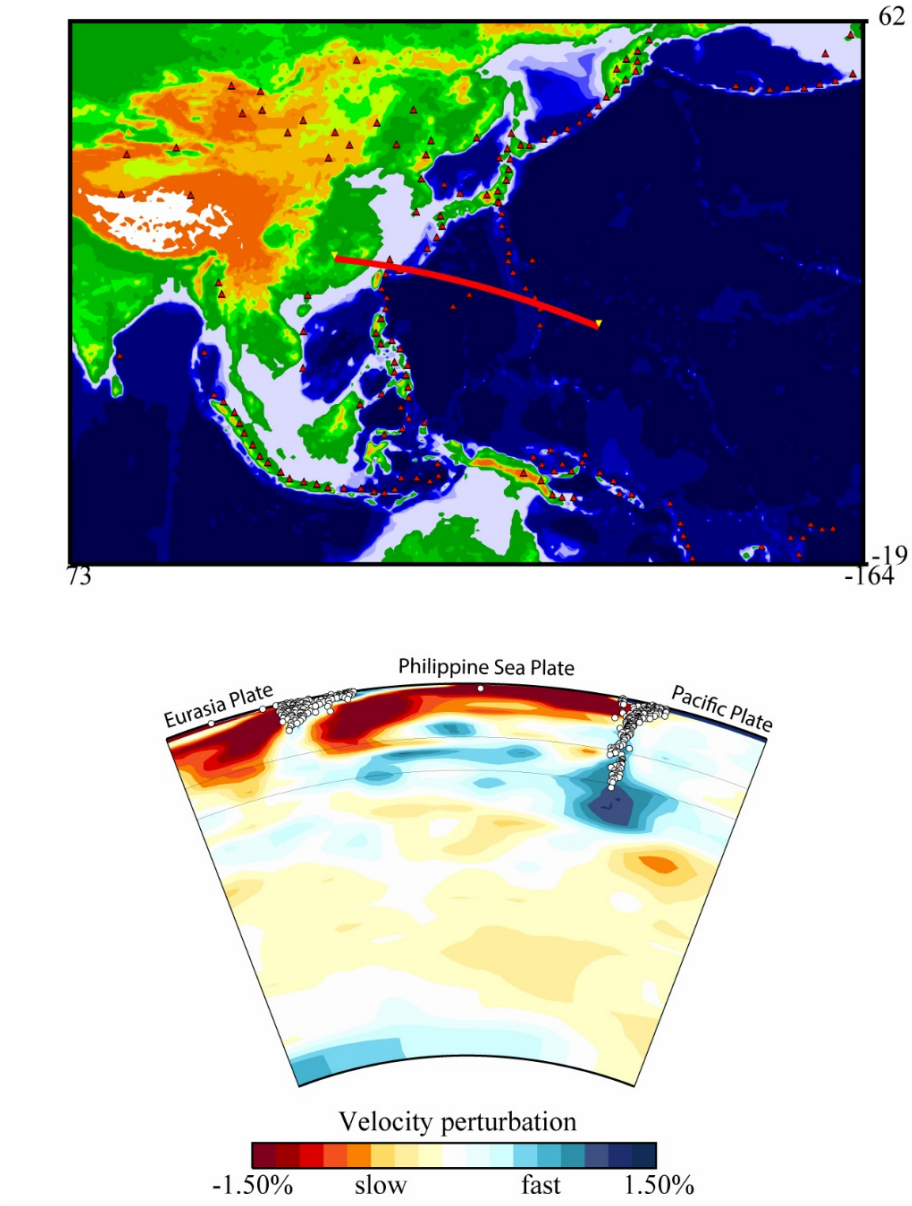

Figure 2. **Global seismic tomography 2-D vertical cross section (bottom) and a cross line on topographic map(up).** The GAP_P4, p-wave tomography model, is applied (Obayashi et al. 2013). Red solid line – cross line of the vertical section; white dots – earthquake focal center.

The models of the WPB suggested thus far can be classified into two main categories: entrapment model (Uyeda and Ben Avraham, 1972; Uyeda and McCabe, 1981; Shih, 1980; Uyeda and McCabe, 1983; Hilde and Lee, 1984) and back-arc-origin model (Lewis et al., 1982; Hall et al., 1995; Hall, 2001; Deschamps and Lallemand, 2002). The traditional thought was the entrapment model that the WPB originated from the entrapment of the Kula-Pacific plate when Mesozoic seafloor became segregated from the Pacific Plate as a result of change in its motion around 45 Ma (Uyeda and Ben Avraham, 1972).

Lewis et al. (1982) challenged this idea and argued that the WPB formed as a result of back-arc basin spreading which implies that there was a subduction force driving the system. Also, Hilde and Lee (1984) who examined the magnetic anomaly in detail suggested that the extension of the WPB which started in NE-SW direction at around 60 Ma suddenly changed to N-S direction roughly between 45 to 40 Ma.

The debate between trapped Mesozoic plate and subduction zone driven back-arc opening continues because the oldest part of the basin is missing as it has been subducted under the Eurasian plate. In spite of such uncertainty, several paleomagnetic reconstruction models have been suggested. It is now generally accepted that the PSP underwent clock-wise rotation during the last 50 Ma or so (Hall et al., 1995; Hall et al., 2002; Yamazaki, 2010; Richter and Ali, 2015). However, much of the early history of the PSP remains unknown. One of the reasons is that the coverage of the previous marine magnetic surveys was not uniform and thus there are important gaps

in our understanding.

Since Hilde and Lee (1984), various geophysical studies [Deschamps and Dominguez, 1999; Okino et al., 2001; Deschamps and Lallemand, 2002; Taylor and Goodliffe, 2004; Deschamps et al., 2008; Horner-johnson and Gordon, 2003] have revealed the motion history of the WPB. However marine magnetic analyses in the area are still controversial with different opinions. Because skewed and weak magnetic anomalies from complex basin formation make it difficult to compare the phase of magnetic anomaly to that of 2-D box model.

This study re-examines the opening of the WPB using previously collected proton precession magnetometer (PPM) magnetic anomaly data. However, unlike the former studies, we include sea-surface marine magnetic anomaly data that are newly added to the database including the shipboard three-component magnetometer (STCM) data which contain three component vectors of magnetic anomaly. It provides a new insight into the overall opening speed and its beginning. Because the vertical component magnetic anomaly which is not affected by horizontal magnetic field variations show the most coherence with its 2-D synthetic model compared to the other previous proton precession magnetic data analysis. The purpose of this re-examination is to better understand the opening style of the WPB. By elucidating the magnetic anomalies within the basin, we may be able to provide new information on the interaction kinematic spreading model of the WPB with surrounding basins during the formative stages of PSP.

Table 1. Kinematic description of previous studies in the WPB.

Spreading phase	Spreading rate	Reference
1	Model : 4.4cm/yr *"Poorly Match"*	Watts et al. (1976)
1	7-15 : 2.5cm/yr 15-18 : 5 - 5.3cm/yr 18-21 : 2.8 - 3.0cm/yr	Shih (1980)
2	used Watts et al (1976) model 4.4cm / yr *"the rate in the main basin was about 9 cm / yr."*	Mrozowski et al. (1982)
2	Model : 4.4cm/yr well match with early stage 1.8 cm/yr well match with late stage	Hilde and Lee (1984)
2	spreading : 54 - 33/30Ma similar to Okino et al (1999) *"Rate of spreading: most of the WPB crust was formed at a half spreading rate of 44km/Ma"*	Deschamps and Lallemand (2002)
Not mentioned	*"slow spreading rate during the later phase of the evolution"*	Okino et al. (1999)
2 (early – late)	Late stage : 1.8 cm / yr Early stage : 4.4 cm / yr	Okino et al. (2003)
2	Late stage : 1.8cm / yr Middle stage : "*faster than 4.4cm / yr"*	Sasaki et al. (2014)

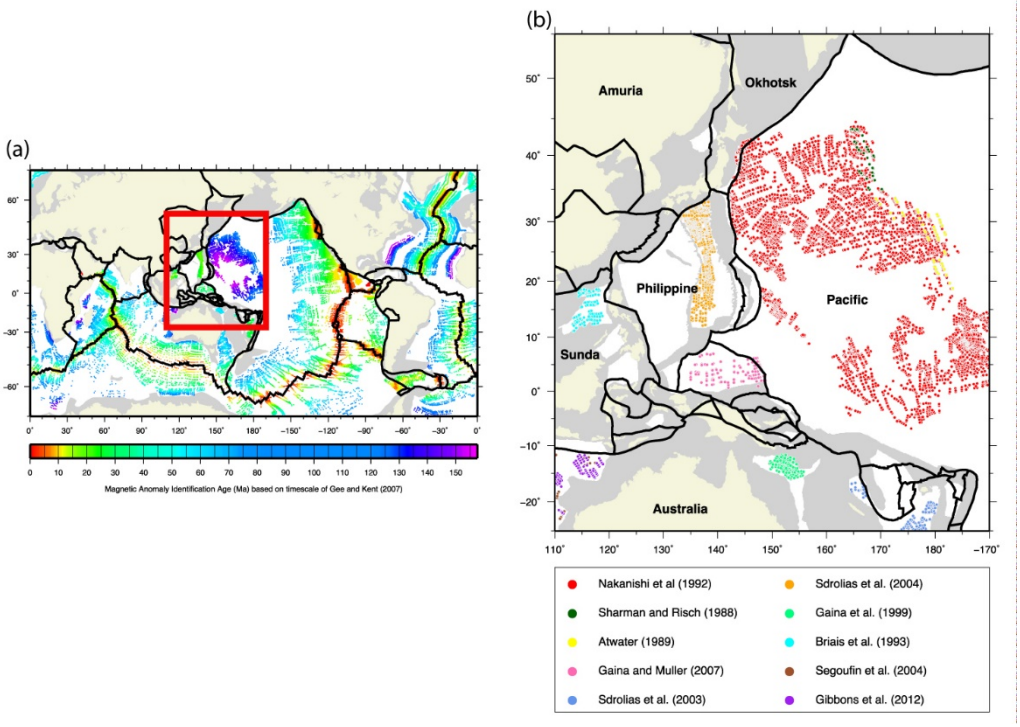

Figure 3. World magnetic anomaly database (Seton et al., 2014). The West Philippine Basin still remains no data because of complex formation.

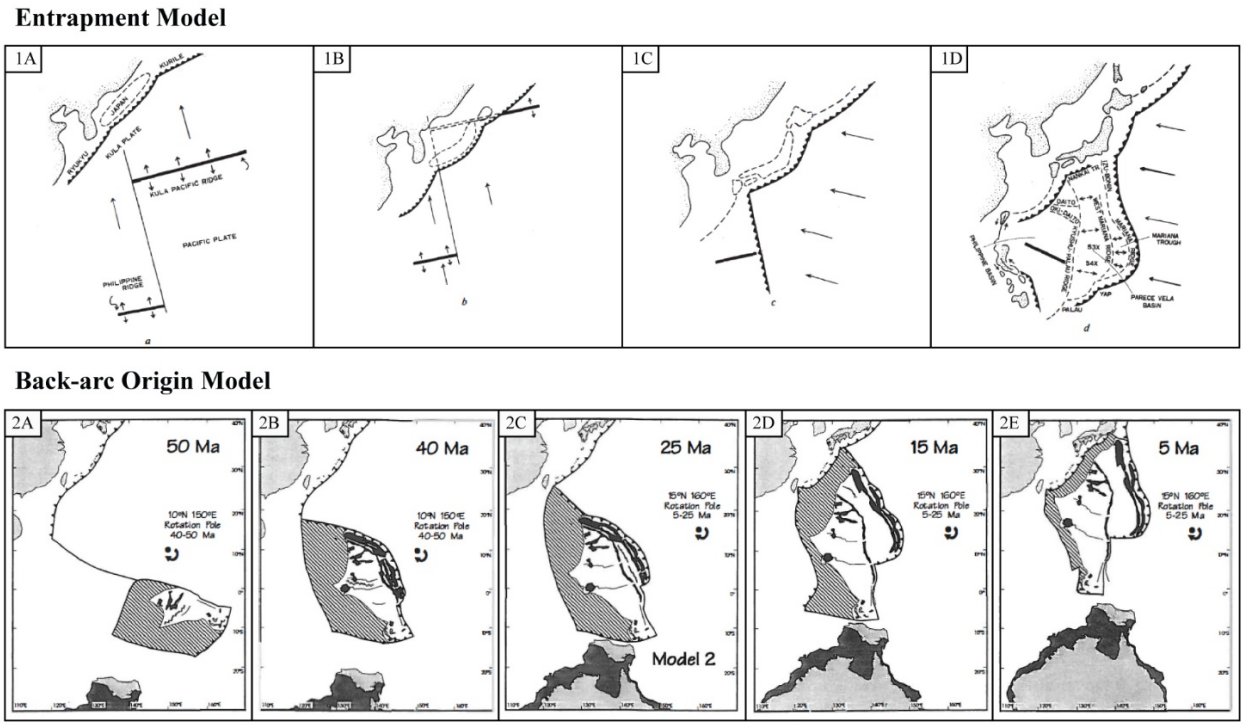

Figure 4. Two different hypothesis suggested by Uyeda and Ben Avraham (1972) (top) and Lewis et al (1982) (bottom).

2. DATA

2.1 Bathymetry data

Bathymetry data were obtained from a shipboard survey and from satellite altimetry. Typically, the bathymetry grid derived from Satellite altimetry is difficult to study detailed tectonic structures caused by geodynamic activities because it has wide data coverage but low resolution. On the other hand, multi-beam bathymetry measured by shipborne echo sounder has narrow coverage but high resolution which is enough to study small tectonic structures.

The high resolution bathymetry study in the WPB was previously conducted by Andrews (1980); Okino and Fujioka (2003); Deschamps and Lallemand (2002); Tayler and goodliffe (2004). However, the data is insufficient to understand overall tectonic features especially in South of the WPB.

In this study, the multi-beam bathymetry collections focused on the poorly investigated region not only to understand connections between magnetic strike and seafloor abyssal hill trend but also to provide important tectonic structure information for finite rotation pole calculation. These data were collected from the Marine Geoscience Data System (MGDS) and Data Research System for Whole Cruise Information (DARWIN) of Japan Agency for Marine-Earth Science and Technology (JAMSTEC) (since 2001). The detailed cruise information was described in Table 1.

2.2 Magnetic data

The PPM data were obtained from National Geophysical Data Center (NGDC) of National Oceanic and Atmospheric Administration (NOAA). Since each PPM dataset that were gathered from 1940s, magnetic anomalies have been surveyed in the WPB by many countries and vessels, resulting in the elaboration and wide acceptance of Plate Tectonics and the reconstruction of the WPB. Despite these efforts, the crude navigation of early datasets and the lack of data in the poorly investigated area results in errant interpretation and large uncertainties in reconstructions.

In recent year, the high resolution STCM data have been updated on DARWIN of JAMSTEC. The datasets were recorded with high resolution gyro compass by 8Hz sampling rate since the ships have been started to collect the information in 2000s. The detailed magnetic dataset information was described in Table 2.

Table 2. Subsequence data category used in this study.

Cruise ID	Platform	Data	Operation start	Overation end	Chief scientist	Source	Publisher
COOK11MV	R/V Melville	MB	20010808	20010817	transit	SIO, USA	NGDC, NOAA
DSDP31GC	D/V GlomarChallenger	PPM	1973-06-15	1973-08-04	KARIG D.E.	SIO, USA	NGDC, NOAA
EW9510	MauriceEwing	MB	1995-09-28	1995-10-15	B. Taylor	LDEO, USA	NGDC, NOAA
GG01	R/V Gagarinskiy	PPM	1988	1988	ZABOLOTNIKOV	IMGG, USSR	NGDC, NOAA
HT90T211	Takuyo	PPM	1990	1991	H. Masayoshi	Japan	NGDC, NOAA
HT90T212	Takuyo	PPM	1990	1990	H. Masayoshi	Japan	NGDC, NOAA
HT90T222	Takuyo	PPM	1990	1990	H. Masayoshi	Japan	NGDC, NOAA
HT94T312	Takuyo	PPM	1994	1994	S. Kasuga	Japan	NGDC, NOAA
HT94T313	Takuyo	PPM	1994	1994	S. Kasuga	Japan	NGDC, NOAA
HT94T321	Takuyo	PPM	1994	1994	T. Omori	Japan	NGDC, NOAA
HT94T322	Takuyo	PPM	1994	1994	T. Omori	Japan	NGDC, NOAA
HT94T323	Takuyo	PPM	1994	1994	T. Omori	Japan	NGDC, NOAA
HT94T324	Takuyo	PPM	1994	1994	T. Omori	Japan	NGDC, NOAA
HT95T343	Takuyo	PPM	1995	1995	S. Kasuga	Japan	NGDC, NOAA
HT95T351	Takuyo	PPM	1995	1995	T. Omori	Japan	NGDC, NOAA
HT95T352	Takuyo	PPM	1995	1995	S. Kasuga	Japan	NGDC, NOAA
HT96T361	Takuyo	PPM	1996	1996	S. Kasuga	Japan	NGDC, NOAA
HT96T362	Takuyo	PPM	1996	1996	S. Kasuga	Japan	NGDC, NOAA
HT96T363	Takuyo	PPM	1996	1996	M. Uchida	Japan	NGDC, NOAA
HT97T353	Takuyo	PPM	1997	1997	Y. Shimohira	Japan	NGDC, NOAA
HT97T354	Takuyo	PPM	1997	1997	K.Kusunoki	Japan	NGDC, NOAA
HT97T355	Takuyo	PPM	1997	1997	Y.Kuroda	Japan	NGDC, NOAA
HT97T391	Takuyo	PPM	1997	1997	N. Shimizu	Japan	NGDC, NOAA

Table 2. *(continued)*

Cruise ID	Platform	Data	Operation start	Operation end	Chief scientist	Source	Publisher
HT97T393	Takuyo	PPM	1997	1997	Y. Kuroda	Japan	NGDC, NOAA
IIOECGS	Pioneer	PPM	1964	1964	Stewart	NOAA, USA	NGDC, NOAA
KM0909	Kilo Moana	MB	2009-03-20	2009-04-09	L. Ren-Chieh	UH, USA	NGDC, NOAA
KM0911	Kilo Moana	MB	2009-05-15	2009-05-20	M. Timothy	UH, USA	NGDC, NOAA
KY09-01_leg1	R/V Kaiyo	MB	2009-02-09	2009-05-11	K. Ando et al.	JAMSTEC,Japan	DARWIN, JAMSTEC
KY12-08	R/V Kaiyo	MB,	2012-05-19	2012-07-08	Y. Ohta	JAMSTEC,Japan	DARWIN, JAMSTEC
MARA11WT	R/V ThomasWashingto	PPM	1979	1979	Shor G.G.	SIO, USA	NGDC, NOAA
MGL0904	Marcus G. Langseth	MB	2009-03-11	2009-03-28	J. Anthony	LDEO, USA	NGDC, NOAA
MGL0904	Marcus G. Langseth	MB	2009-03-11	2009-03-28	J. Anthony	LDEO, USA	NGDC, NOAA
MGLN37MV	R/V Melville	MB	2008-04-28	2008-05-03	Transit	SIO, USA	NGDC, NOAA
MR01-K05_l12	R/V Mirai	MB	2001-09-20	2001-11-05	Y. Kuroda, K. Mizuno	JAMSTEC,Japan	DARWIN, JAMSTEC
MR02-K04	R/V Mirai	MB, STCM	2002-06-24	2002-08-22	Y.Kuroda, H. Hase	JAMSTEC,Japan	DARWIN, JAMSTEC
MR03-K03leg1	R/V Mirai	MB, STCM	2003-06-07	2003-07-30	H. Hase, S. Minato	JAMSTEC,Japan	DARWIN, JAMSTEC
MR04-03_leg1	R/V Mirai	MB, STCM	2004-06-06	2004-07-02	I. Ueki	JAMSTEC,Japan	DARWIN, JAMSTEC
MR04-03_leg2	R/V Mirai	MB, STCM	2004-07-03	2004-08-03	H. Hase	JAMSTEC,Japan	DARWIN, JAMSTEC
MR05-03_leg1	R/V Mirai	MB	2005-07-03	2005-07-25	K. Ando	JAMSTEC,Japan	DARWIN, JAMSTEC
MR06-05_leg3	R/V Mirai	MB, STCM	2006-12-14	2007-01-19	Y. Kashino	JAMSTEC,Japan	DARWIN, JAMSTEC
MR07-07_leg1	R/V Mirai	MB, STCM	2007-12-27	2008-01-25	Y. Kashino	JAMSTEC,Japan	DARWIN, JAMSTEC
MR08-02	R/V Mirai	MB, STCM	2008-05-26	2008-06-30	K. Yoneyama	JAMSTEC,Japan	DARWIN, JAMSTEC
MR10-02	R/V Mirai	MB	2010-04-06	2010-05-02	K. Ando	JAMSTEC,Japan	DARWIN, JAMSTEC
MR11-06	R/V Mirai	MB, STCM	2011-08-13	2011-09-20	Y. Kashino	JAMSTEC,Japan	DARWIN, JAMSTEC
MR13-01	R/V Mirai	MB, STCM	2013-02-18	2013-03-28	Y. Kashino	JAMSTEC,Japan	DARWIN, JAMSTEC
RAMA11WT	R/V ThomasWashingto	PPM	1981-03-10	1981-03-25	L. Dale Bibee	SIO, USA	NGDC, NOAA

Table 2. *(continued)*

Cruise ID	Platform	Data	Operation start	Operation end	Chief scientist	Source	Publisher
RC1107	R/V Robert D. Conrad	PPM	1967	1967	J. HIERTZLER	LDEO, USA	NGDC, NOAA
RC1711	R/V Robert D. Conrad	PPM	1974-09-16	1974-10-14	Watts, Anthony	LDEO, USA	NGDC, NOAA
RC2006	R/V Robert D. Conrad	PPM	1976	1976	Hayes, Dennis	LDEO, USA	NGDC, NOAA
RR1005	R/V Roger Revelle	MB	2010-04-06	2010-04-28	W. Peter	SIO, USA	NGDC, NOAA
RR1006	R/V Roger Revelle	MB	2010-05-06	2010-05-29	M. James	SIO, USA	NGDC, NOAA
RR1014	R/V Roger Revelle	MB	2010-10-12	2010-10-24	O. Mike	SIO, USA	NGDC, NOAA
RR1105	R/V Roger Revelle	MB	2011-03-24	2011-04-16	W. Peter	SIO, USA	NGDC, NOAA
RR1208	R/V Roger Revelle	MB	2012-06-28	2012-07-17	A. Bruce	SIO, USA	NGDC, NOAA
RR1308	R/V Roger Revelle	MB	2013-06-12	2013-06-26	W. Caitlin	SIO, USA	NGDC, NOAA
RR1313	R/V Roger Revelle	MB	2013-09-08	2013-10-03	R. Yair	SIO, USA	NGDC, NOAA
RR1403	R/V Roger Revelle	MB	2014-04-14	2014-04-19	A. Bruce	SIO, USA	NGDC, NOAA
TSDY05WT,	R/V ThomasWashingto	PPM	1973-09-13	1973-10-06	Karig, Daniel	SIO, USA	NGDC, NOAA
TSDY07WT,	R/V ThomasWashingto	PPM	1973	1973	Bezdek H.	SIO, USA	NGDC, NOAA
UM63	Umitaka Maru	PPM	1963	1964	unknown	Univ.Tokyo, Japan	NGDC, NOAA
UM66-d	Umitaka Maru	PPM	1967	1967	unknown	Univ.Tokyo, Japan	NGDC, NOAA
V3310	Vema	PPM	1976-08-27	1976-09-19	Truchan	LDEO, USA	NGDC, NOAA
V3505	Vema	PPM	1978-06-04	1978-07-02	Hayes	LDEO, USA	NGDC, NOAA
VA16	Valdivia	PPM	1977	1977	K.Hinz	BG	NGDC, NOAA
YK02-07_Leg1	R/V Yokosuka	STCM	2002-09-25	2002-10-20	Soh Wonn	JAMSTEC,Japan	DARWIN, JAMSTEC
YK10-14	R/V Yokosuka	MB, STCM	2010-10-22	2010-11-09	O. Ishizuka	JAMSTEC,Japan	DARWIN, JAMSTEC
ZHNG04RR	R/V Roger Revelle	MB	2005-03-29	2005-04-15	transit	SIO, USA	NGDC, NOAA

3. METHODS

3.1 Multi-beam bathymetry

The data from JAMSTEC which consist of longitude, latitude and corrected ocean depth were easy to make shaded bathymetry grid however the MGDS data that contains binary files were processed and converted to xyz format using MB-system. ETOPO1 was mingled into uninvestigated area (Fig. 5). We applied the bathymetry interpretation method [Dauteuil and Brun, 1996; Dauteuil et al., 2001; Dauteuil and Brun, 1993; Spencer et al., 1997]. The illustration of abyssal hill strikes from former studies [Okino and Fujioka, 2003; Deschamps and Lallemand, 2002; Taylor and Goodliffe, 2004] were merged into the description of this study (Fig. 14)

3.2 Magnetic anomaly

3.2.1 Proton Precession Magnetometer

The PPM data that measures absolute total intensity magnetic field are sum of the Earth magnetic field and remnant magnetization of the oceanic crust. Thus, the Earth magnetic field is removed using the International Geomagnetic Reference Field (IGRF, B_{igrf}) model to get residual magnetic anomaly (ΔB) originated from oceanic crust.

$$\Delta B = B_{raw} - B_{igrf}$$

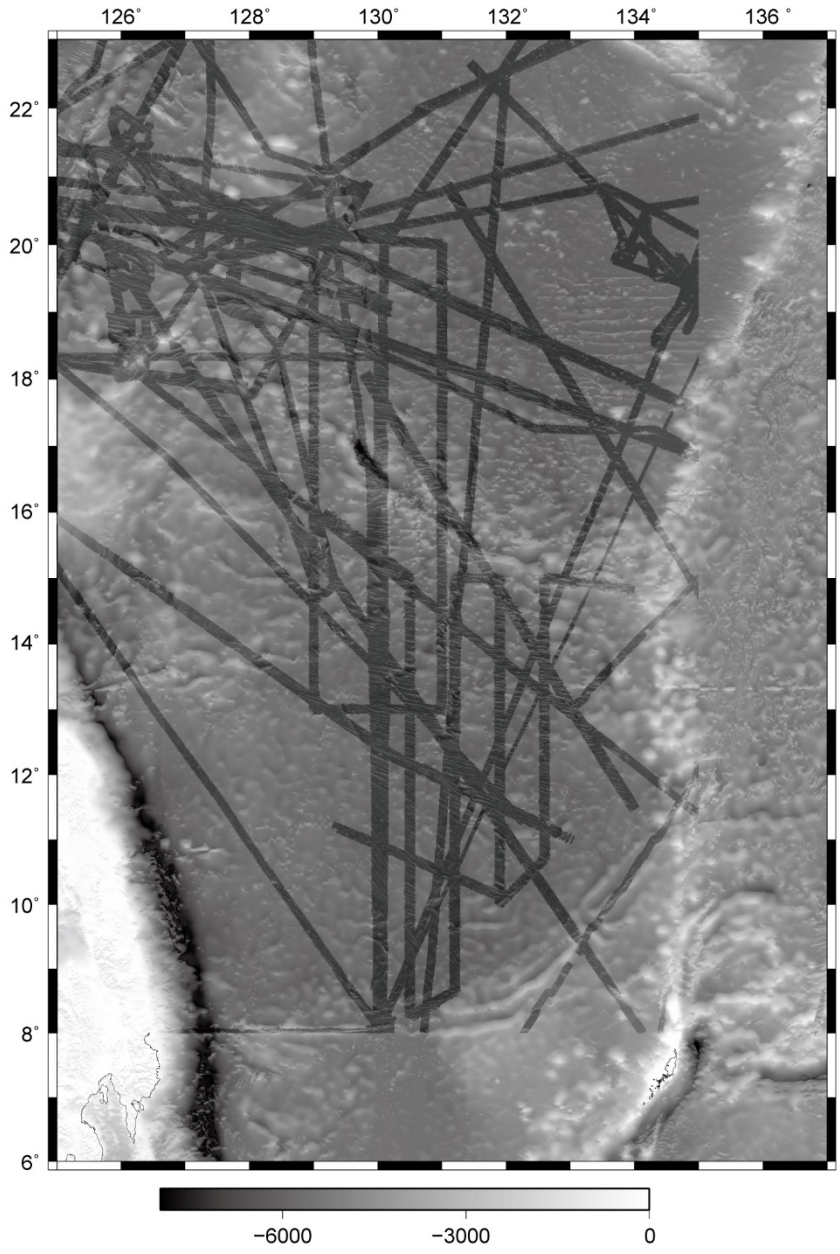

Figure 5. The shaded subsequence shipborne high-resolution bathymetry grid (dark gray). ETOPO1, 1-arc minute resolution global satellite derived bathymetry was plotted for uninvestigated area (light gray background).

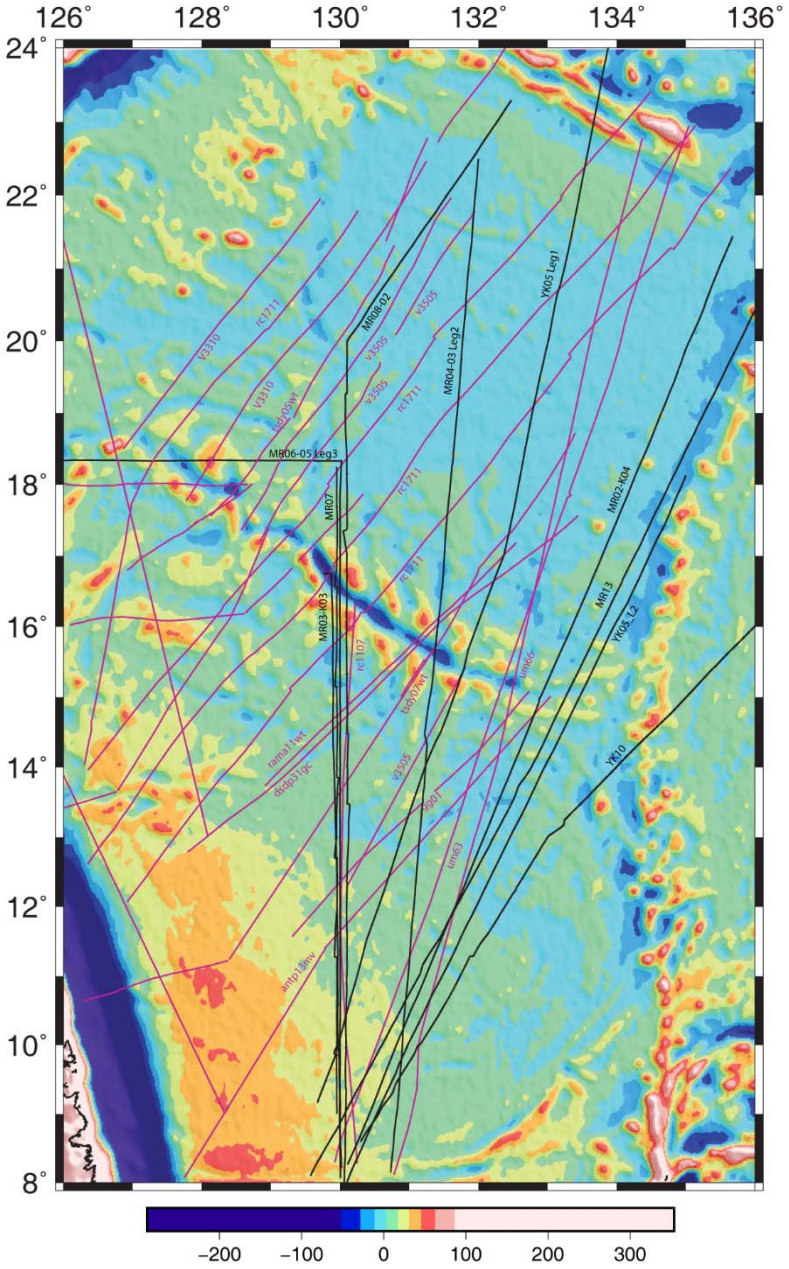

Figure 6. Marine magnetic survey tracks used in this study. PPM survey track of solid purple line, STCM survey track of solid black line. The global marine gravity grid (Sandwell and Smith, 2009) was plotted to the background. The unit of gravity index is milli-gal (mgal)

Each dataset was evenly interpolated by 0.2 km spaced and band pass filtering of 3-10km cutoff wavelength was applied. Because the susceptibility in oceanic crust is generally originated from pillow basalt layer (2A) in ophiolite complex which usually forms 0.5-1.0 km thickness from seafloor (Dilek and Furnes, 2014). The synthetic magnetic 2-D box model were calculated using half spreading rate of 4.4 cm/yr, 6 km water depth, magnetization intensity of 5 A/m, and 1 km thick extrusive basalt layer.

3.2.2 STCM data processing

STCM which observes relative vector magnetic anomalies is an efficient apparatus because the sensor is able to obtain data without additional deployment and manipulations, which differs from PPM method requiring rear towing on the ship. Also, the vertical component magnetic anomaly that is not affected by horizontal magnetic field variations shows the most coherence with its synthetic model among the other previous magnetic data analyses. However, the signal processing of the STCM data is complicated because the data include more information such as not only just sum of the Earth magnetic field and magnetic anomaly but also position of the ship and its induced magnetization.

The basic concept of data processing flow chart used in this study is shown in figure 7. The erroneous data were removed for preprocessing of ship magnetization coefficients calculation by roll and pitch angles of ± 45˚ and yaw variation of 20 deg/sec. In addition, the raw fluxgate data which exceeded over than ± 60000 nT for X

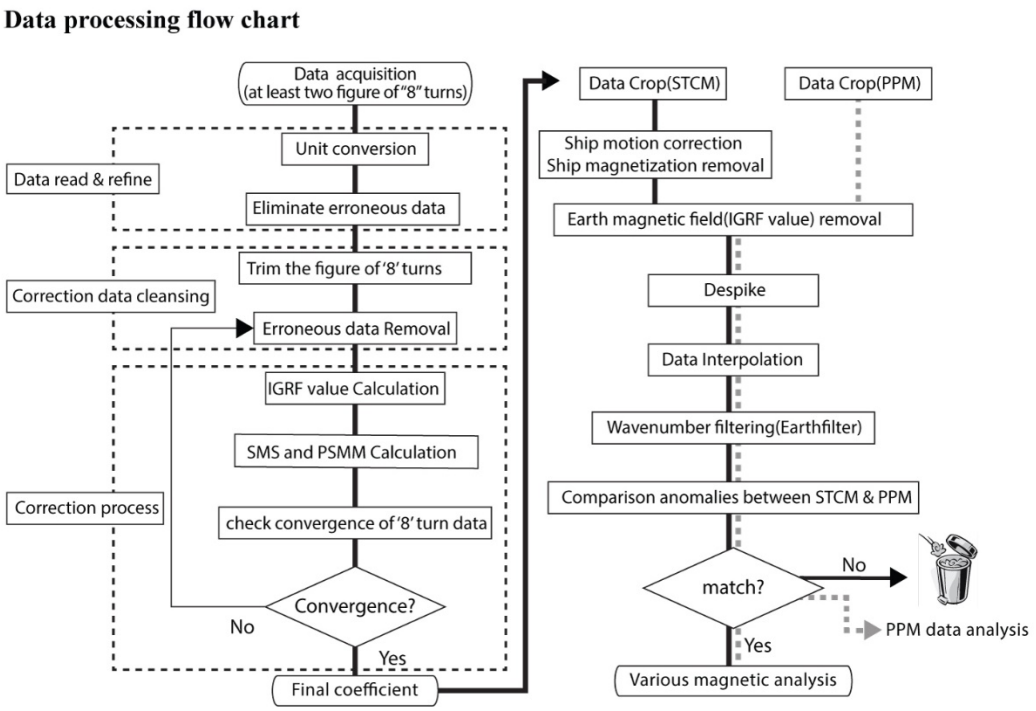

Figure 7. STCM data processing flowchart. Gray dot line of PPM data processing flow chart

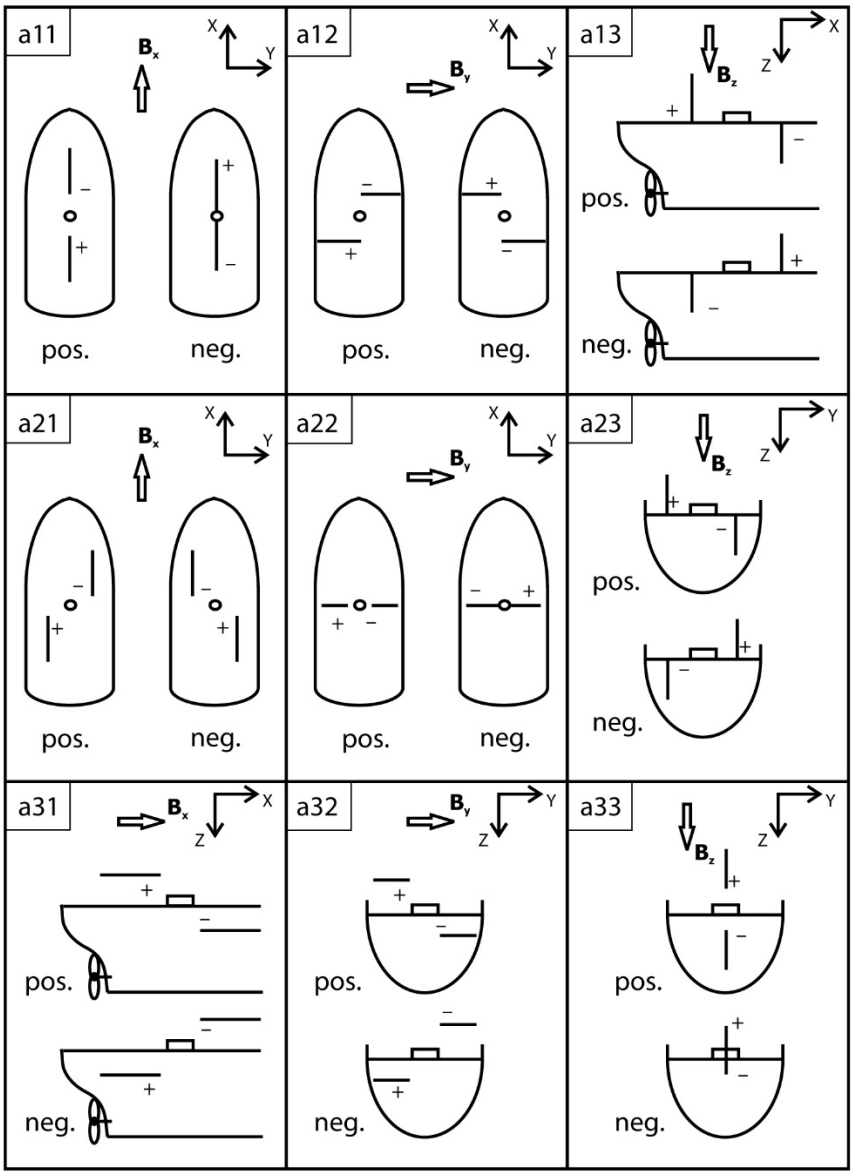

Figure 8. Bars of induction and their relation to the sign of the coefficients for the induced ship's field (König, 2006)

and Y components and over than ± 80000 nT for Z component were removed. The magnetization coefficient matrix was inverted by normal equation of least square method from several times of figure of eight turns from each cruise (Isezaki, 1986). The observed STCM data can be described as

$$H_{ob} = F + H_i + H_p \quad (1)$$

H_{ob} is observed magnetic field, F is the Earth magnetic field, H_i is induced magnetic field due to the magnetization of the ship under the influence of the ambient geomagnetic field. H_p is permanent magnetic as measured in each of the directions of the ship's coordinate system. H_i can be expressed to linear equation, thus,

$$H_i = AF \quad (2)$$

Because the values were changed by magnetic field intensity. The A, 3X3 matrix, indicates magnetic susceptibility of the ship. The F value can be described as (RPY)F where R is roll, P is pitch, Y is yaw. Because H_{ob} is varied by roll, pitch, yaw variation of the ship. Therefore, the equation can be expressed as

$$H_{ob} = (A + 1)RPYF + H_p \quad (3)$$

The known values are Hob, RPY, and F. For easy computation, (A+1) can be express to A. So, the linear equation is expressed as

$$H_{ob} = ARPYF + H_p \quad (4)$$

Following the equation (4) the geomagnetic field F can be described as

$$RPYF = BH_{ob} + H_p \tag{5}$$

The equation (5) can be calculated using least square method

$$\mathrm{RPYF} \times H_{ob}^{-1} = P \tag{6}$$

To solve equation (6), $\mathrm{H_{ob}^{-1}}$ can be express as $= \left(\mathrm{H_{ob}^{T}} H_{ob}\right)^{-1} H_{ob}^{T}$ using least square method normal equation. Thus, the matrix P can be solved using the equation (7)

$$\mathrm{RPYF} \times \left(\mathrm{H_{ob}^{T}} H_{ob}\right)^{-1} H_{ob}^{T} = P \tag{7}$$

The value P consist of 3x4 matrix which can be expressed as

$$P = \begin{pmatrix} a_{11} & a_{12} & a_{13} & H_{px} \\ a_{21} & a_{22} & a_{23} & H_{py} \\ a_{31} & a_{32} & a_{33} & H_{pz} \end{pmatrix}$$

a_{ij} (i,j = 1, 2, 3) indicates ship magnetic susceptibility matrix, H_{pk} (k = x, y, z) describes permanent magnetization vector. Figure 8 describes the bars of induction and their relation to the sign of the coefficients for the induced ship's field (König, 2006).

From the calculated coefficient matrix, the corrected magnetic field $\mathrm{H_{corr}}$ can be computed using the equation (8). Thus,

$$\mathrm{H_{corr}} = (RPY)^{-1} P H_{ob} \tag{8}$$

When there are no data of eight turn on that cruise, we used the magnetic coefficients previously computed from proximate cruise because if the STCM sensor was not be

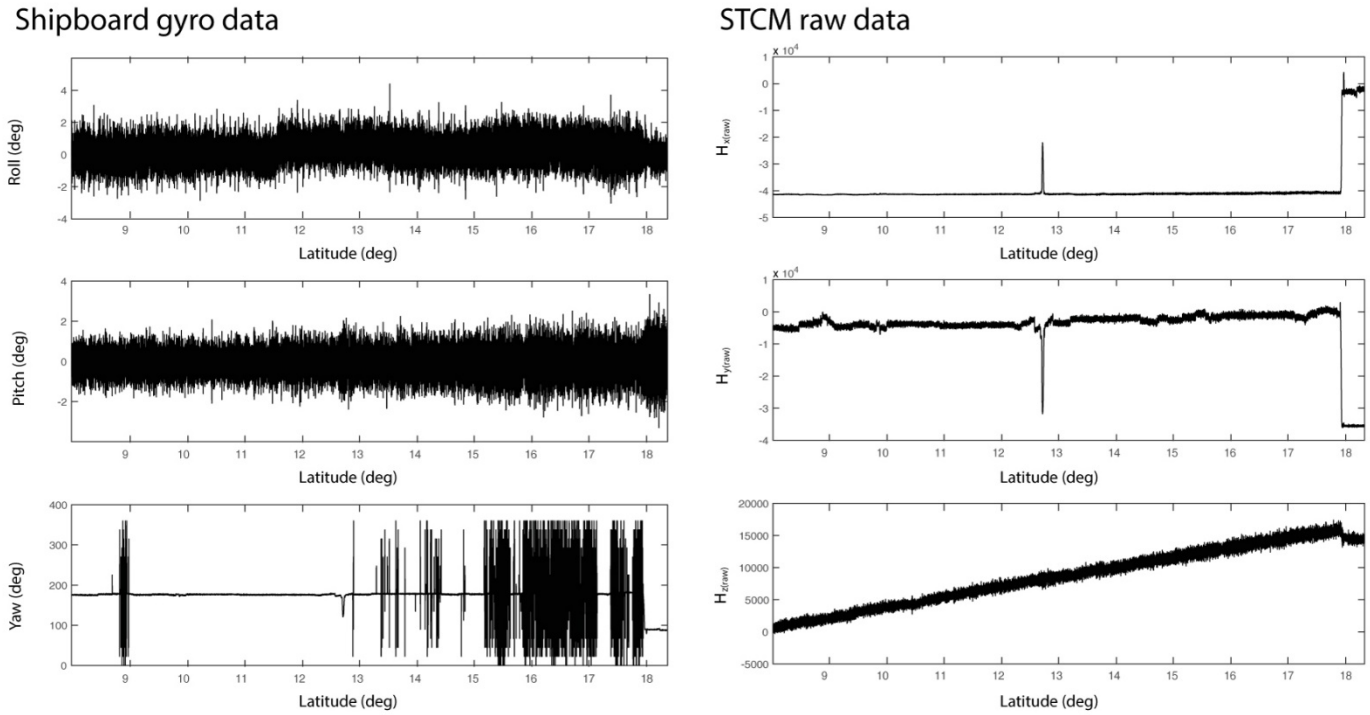

Figure 9. Raw STCM data of the Cruise MR06-05 Leg3. The dataset is composed of navigation, shipborne gyro and STCM data. The x-axis is latitude in degree**.**

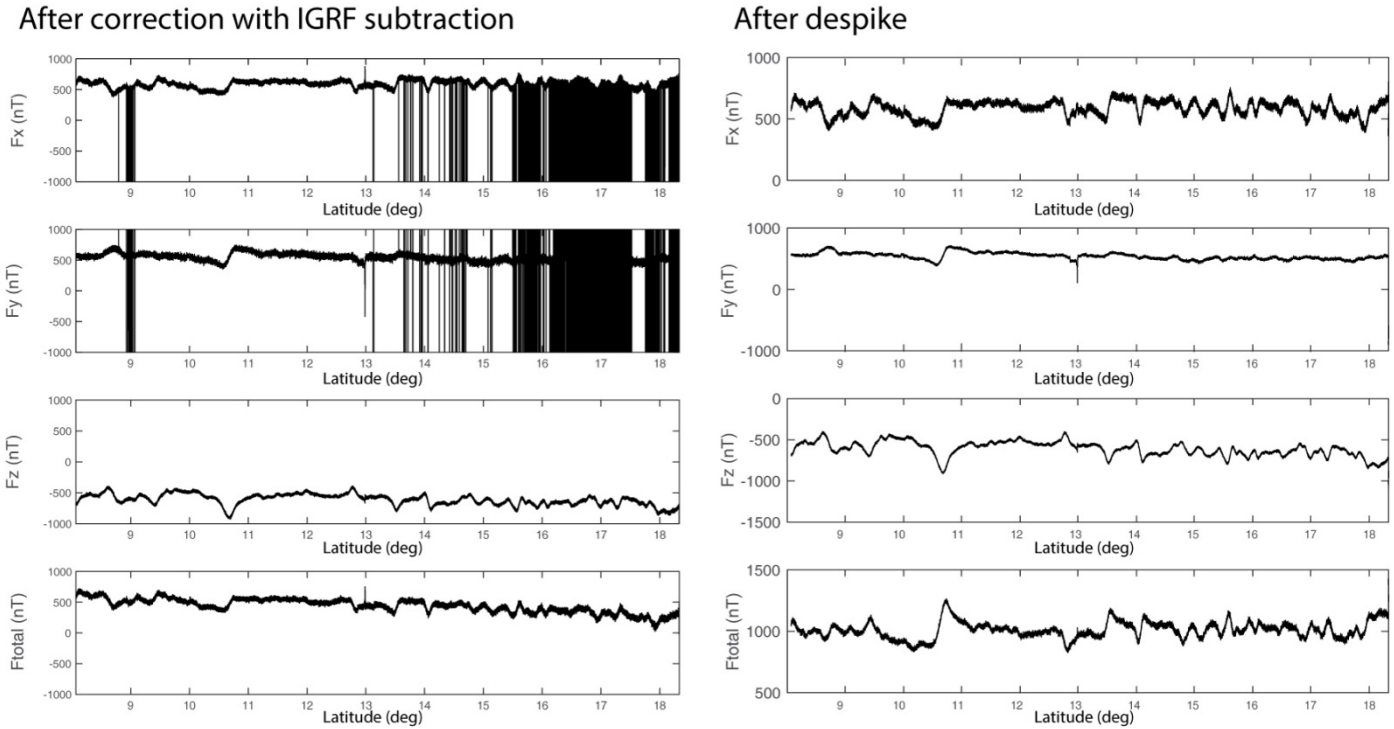

Figure 10. Corrected STCM data of Cruise MR06-05 Leg3 continued from the figure 9. The dataset is composed of navigation, shipborne gyro and STCM data. The x-axis is latitude in degree**.**

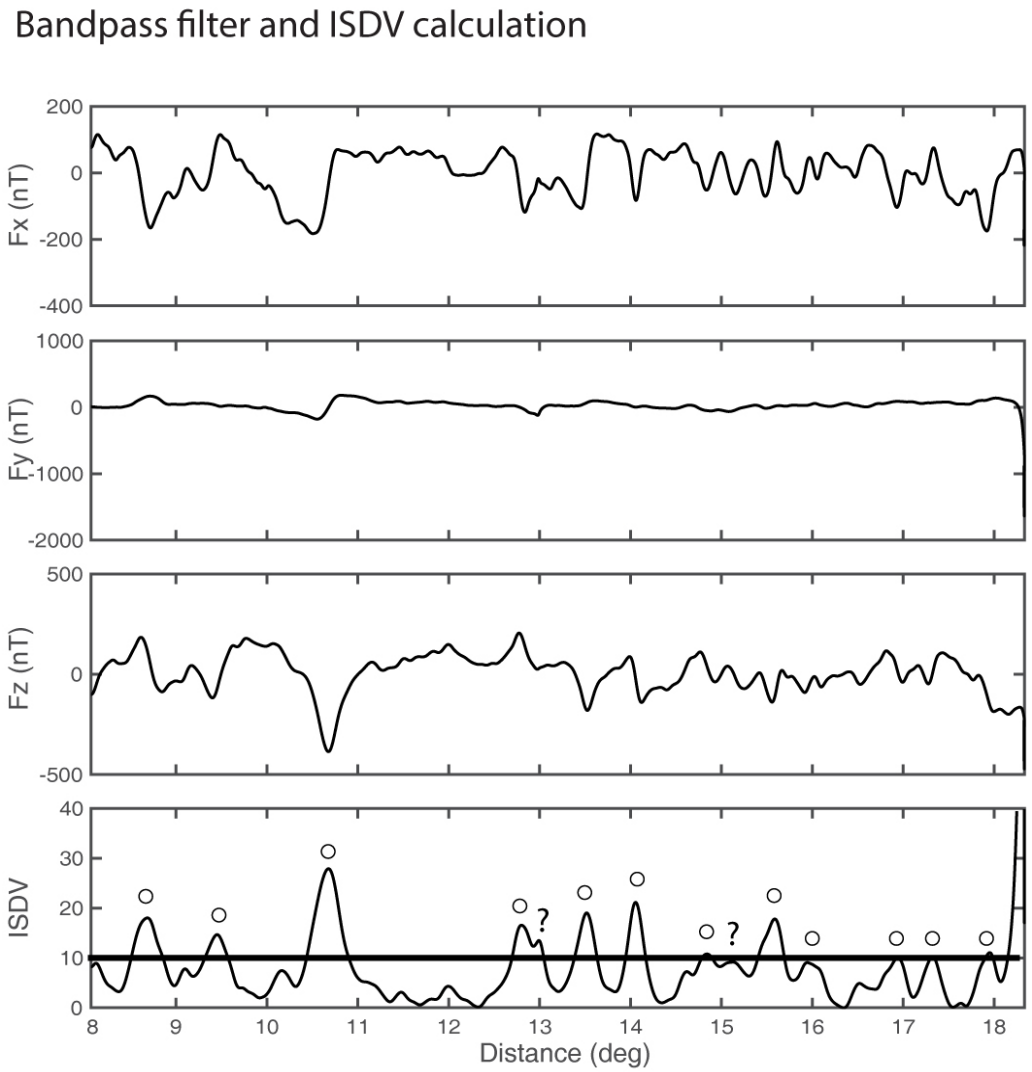

Figure 11. Refined data by bandpass filtering and ISDV calculation continued from the figure 10. Circle is identified magnetic boundary. Question mark is unknown signal. Black solid line on ISDV graph is limit amplitude for detecting magnetic boundaries.

replaced or the vessel was not modified, the main coefficients of ship magnetization is likely to show tiny variation (Nogi and Kaminuma, 1999).

STCM data relatively have more noise which made up of very short wave-length compared to PPM data. Also, magnetic data are affected by long wavelength of diurnal variation. To remove these noises from the signal, bandpass filtering (3-10 km) (Schouten, and McCamy, 1972) was applied to the calculated magnetic anomaly after the spiky noise was removed by despike function with data interpolation by 0.2 km interval along the ship-track line.

In order to test the validity of the STCM data, usually STCM are operated with PPM. However, most of the STCM surveys were not performed with PPM survey. Instead of collecting the total magnetic field data for validity test, so, the magnetic boundary strike diagrams (MBSD) were computed from the intensity of the spatial differential vectors (ISDV) (Seama et al., 1993) (Fig. 11).

The ISDV equation can be expressed as

$$\left|\frac{\partial H}{\partial P}\right| = \sqrt{\left(\frac{\partial H_x}{\partial P}\right)^2 + \left(\frac{\partial H_y}{\partial P}\right)^2 + \left(\frac{\partial H_z}{\partial P}\right)^2} \quad (9)$$

P is distance between each point, H_x, H_y, H_z is magnetic anomalies calculated from STCM data. The calculated STCM magnetic anomalies are compared with 2-D box vertical anomaly model [Nabighian, 1972; Korenaga, 1995] which were postulated half spreading rate of 4.4 cm/yr, 6 km water depth, magnetization intensity of 5 A/m, and 1 km thick extrusive basalt layer (Fig. 12). The magnetic distortion on the vertical

component synthetic model was not considered because the vertical component of magnetic anomaly remains unaffected by magnetic bias from spreading axis change. The detailed STCM survey track and its corrected three component anomalies with ISDV are described between Fig. 18 to Fig. 28.

3.2.3 Euler pole computation

The finite rotation poles for plate reconstruction provide many kinematic information of the plate. Also, the paleo-plate-motion can be effectively simulated by the plate uncertainty method (Hellinger, 1981; Chang et al., 1990; Cox and Hart, 1986).

Finite rotation poles for WPB extension were calculated using the magnetic isochrons and multi-beam bathymetry. The segments of the magnetic anomaly picks were bordered by identified non-transform discontinuities (NTDs) in the east part and transform fault (TF) in the west part of the CBR. The Euler pole calculation was conducted with Gplates version 1.5.0 which is powerful graphic user interface software for tectonic reconstruction (Müller et al., 2011). The computed rotation poles between 22y – 17y (49-36 Ma) were described in the table 2 and figure 15.

Recent paleo-magnetic studies in the WPB and marine geophysical study in the Shikoku and the Parece-Vela Basin were applied to calculate stage poles for the WPB drift motion after the extension was stopped in 26Ma (Fig. 16). Because it is unknown examining marine magnetic survey when some portion of a plate were subducted or a plate were drifted without opening process.

Table 3. Finite rotation poles in different spreading stages of the WPB.

Isochron	Longitude(deg)	Latitude(deg)	Rotation Angle(deg)	conf. level
chron 17y (36.5 Ma)	178.4154398	17.59315781	1.39794613	0.95
chron 18y (38 Ma)	169.7935844	17.80221541	3.693883536	0.95
chron 19y (40 Ma)	-155.3913785	-1.079640905	3.833670847	0.95
chron 20y (42 Ma)	-166.5540418	-4.434086733	5.247737444	0.95
chron 20o (43 Ma)	-143.5081261	-19.48137434	5.916972179	0.95
chron 21y (46 Ma)	-84.04090603	-22.8196516	16.23106875	0.95
chron 22y (49 Ma)	-78.65365849	-20.8410912	25.47592459	0.95

Figure 12. Correlations between vertical component synthetic magnetic anomaly and STCM profiles in the WPB. STCM data of 10 cruises were investigated to understand the history of the basin extension. The synthetic 2-D box model (top) presumed half spreading rate of 4.4 cm/yr, 5 A/m magnetization intensity of 1km thick extrusive basalt layer and 6km water-depth with 0.5km sampling rate. The geomagnetic polarity timescale by Gradstein et al. (2004) was applied. Thick solid line is latitude of Central Basin Ridge, and dotted line is identified magnetic isochrons.

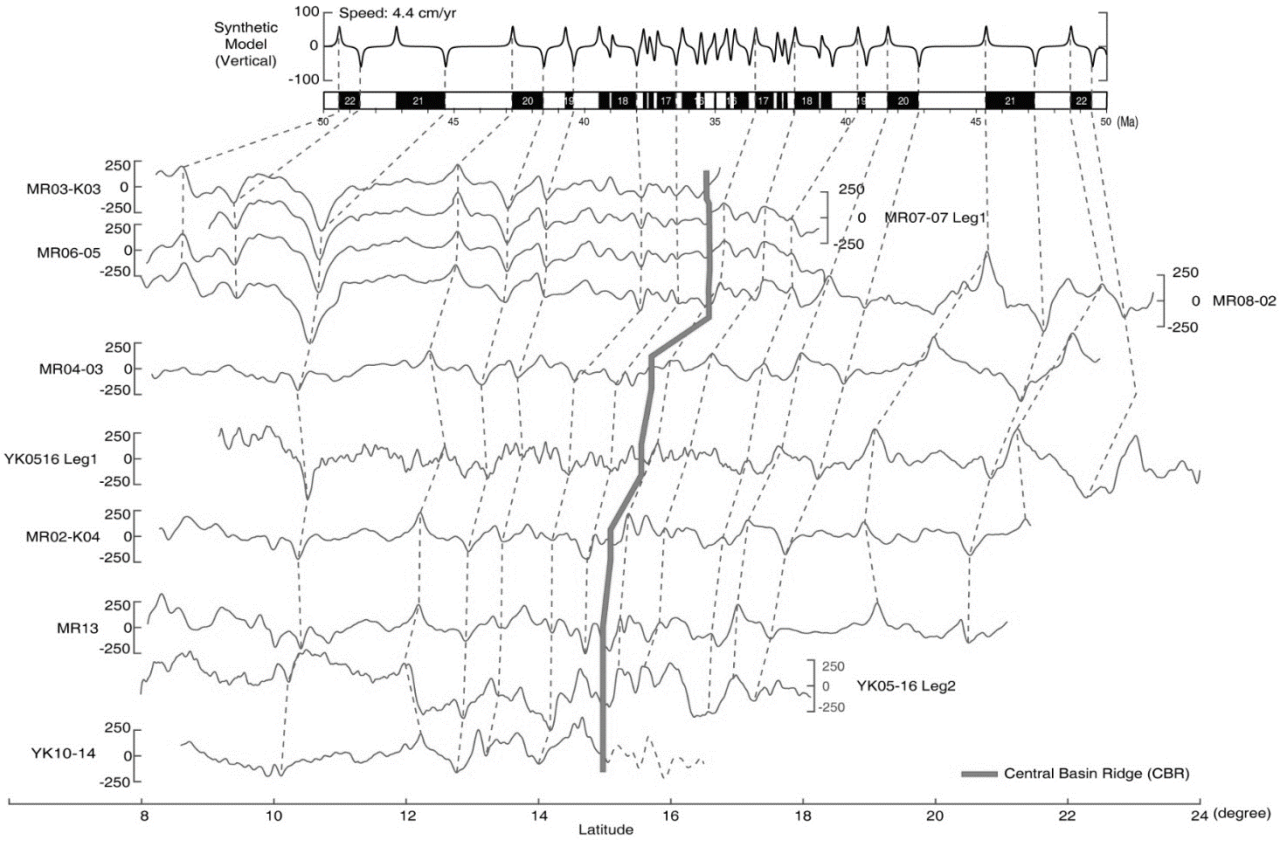
Synthetic Model (Vertical)
Speed: 4.4 cm/yr
100
0
-100
22
21
20
19
18
17
16
15
18
17
18
19
20
21
22
50
45
40
35
40
45
50 (Ma)
MR03-K03
MR06-05
MR04-03
YK0516 Leg1
MR02-K04
MR13
YK10-14
MR07-07 Leg1
MR08-02
YK05-16 Leg2
250
0
-250
Central Basin Ridge (CBR)
8
10
12
14
16
18
20
22
24 (degree)
Latitude

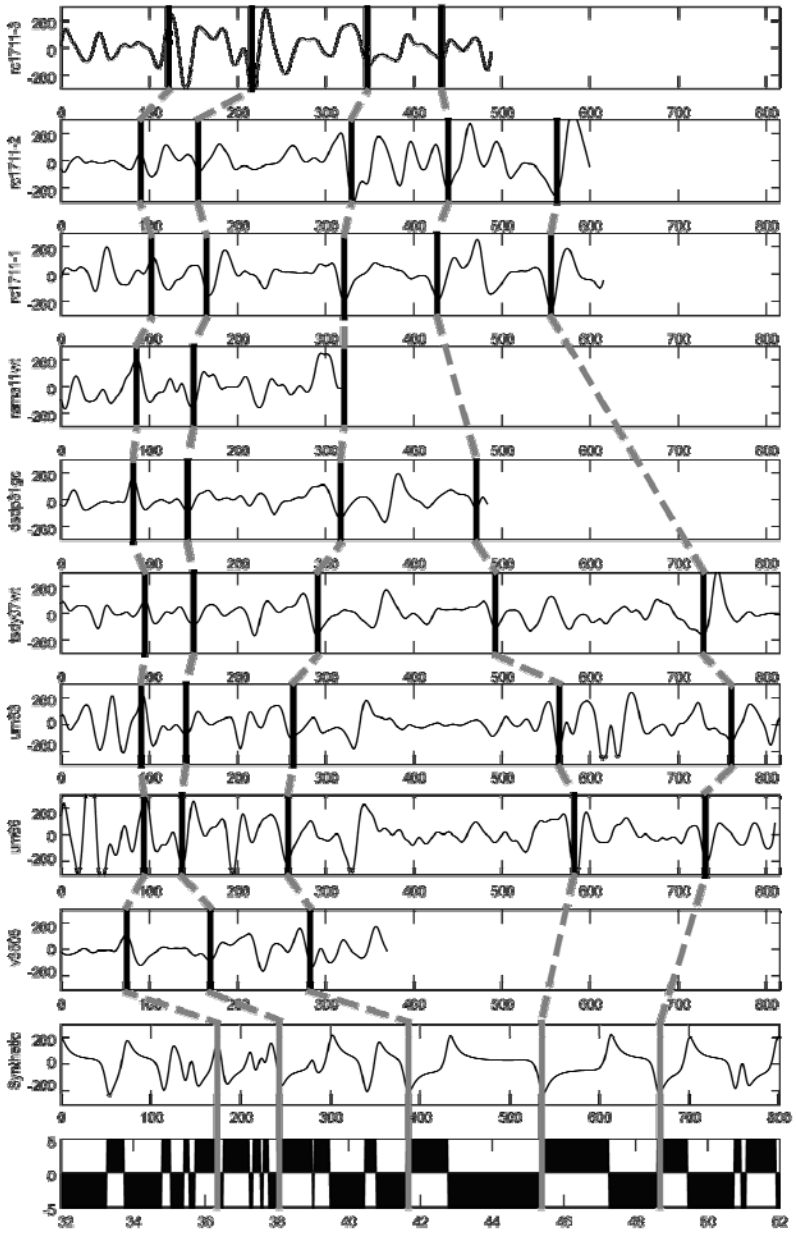

Figure 13. PPM magnetic anomaly and 2-D synthetic magnetic model. The total intensity synthetic model (bottom) presumed half spreading rate of 4.4 cm/yr, 5 A/m magnetization intensity of 1km thick extrusive basalt layer and 6km water-depth with 0.5km sampling rate. The geomagnetic polarity timescale by Gradstein et al. (2004) was applied.

4. RESULTS

The identifications of magnetic isochrons from PPM and STCM data were difficult that the most of the magnetic survey lines were not investigated perpendicular to spreading axis. The combined analysis with high resolution bathymetry grid gave good insight to understand spreading process and magnetic anomaly identification.

For each STCM profiles, the shapes of vertical component magnetic anomalies have good correlation with that of 2-D box model compared to the total component magnetic anomaly (Fig. 12 and 13). The magnetic isochrons can be identified between chron 22y – 17y (49-36Ma). However, the observed magnetic anomaly compared with the synthetic model cannot be identified not only between chron 17y to the CBR but also between chron 22y to subducted part.

The strike directions of MBSD computed from ISDV are likely to agree with the directions of the identified magnetic lineation which changes gradually in clockwise from the E-W to NNW-SSE far from the CBR (Fig. 14). Also, the directions of the seafloor abyssal hill strikes are likely to agree with that of MBSDs. However, few MBSDs were not correlated with magnetic strike boundaries. For example, few MBSDs in the (Coordinate) were displayed on the fracture zone where is located in the middle of the magnetic blocks. Also, MBSDs in the north of Oki Daito Escarpment (ODE) were not matched with seafloor abyssal hill strikes in the same area (Fig. 14).

Figure 14. Combined analysises with strikes of topographic abyssal hill and various magnetic studies in WPB. The global marine gravity grid (Sandwell and Smith, 2009) were used to background. Red solid lines is determined magnetic isochrons by combined study. Black solid line – topographic abyssal hills, white solid line – Magnetic Boundary Strike Diagram (MBSD).

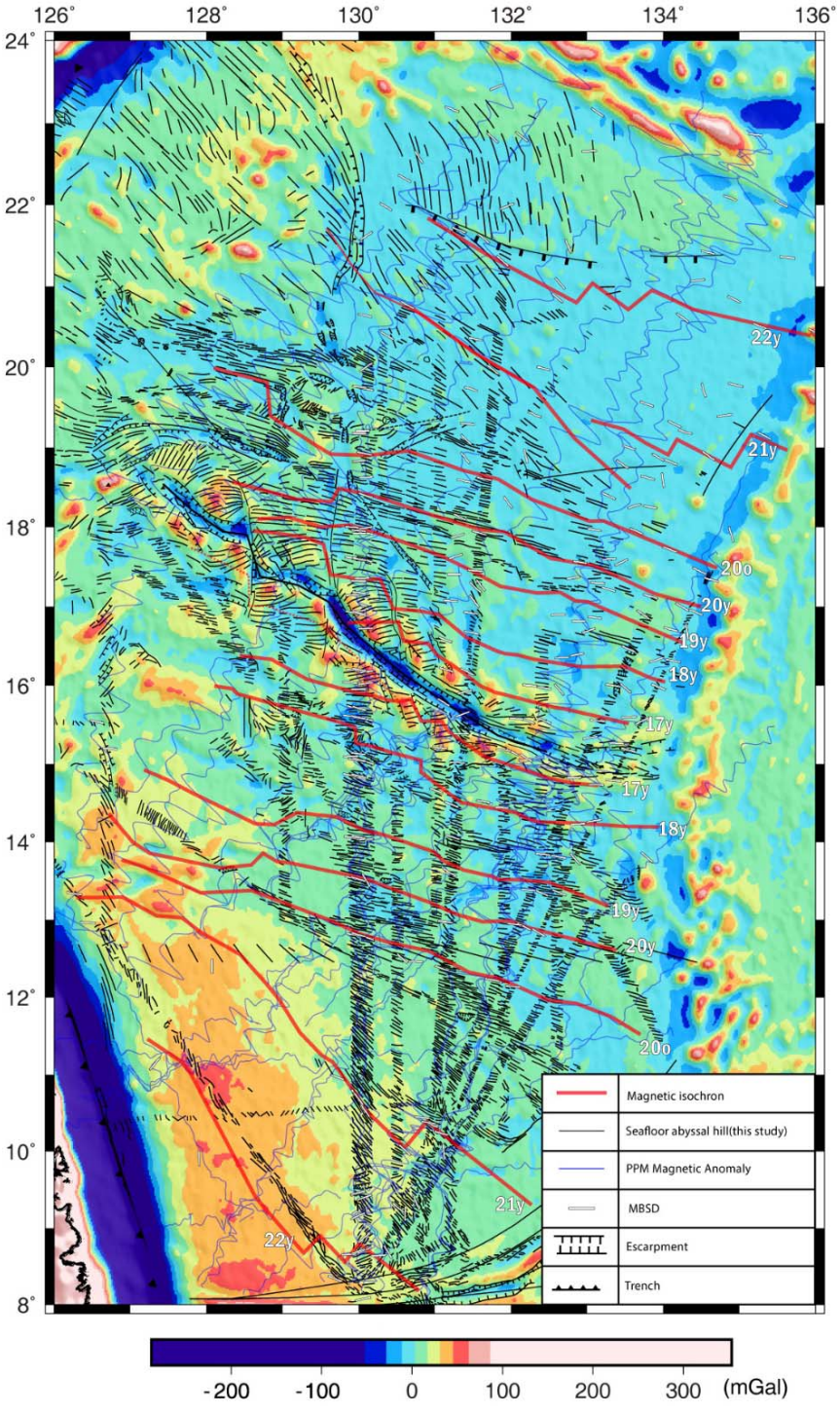
126°
128°
130°
132°
134°
136°
24°
22°
20°
18°
16°
14°
12°
10°
8°
22y
21y
20o
20y
19y
18y
17y
17y
18y
19y
20y
20o
21y
22y
Magnetic isochron
Seafloor abyssal hill(this study)
PPM Magnetic Anomaly
MBSD
Escarpment
Trench
-200
-100
0
100
200
300
(mGal)

Time dependent absolute driving speed of each model were illustrated in Figure 15. We applied the computed rotation poles and the reference models from former paleo-magnetic studies (Hall et al., 1995; Hall, 2002) and marine magnetic surveys for the opening of SB and PVB (Sdrolias et al., 2004) to the first model (Fig. 16-A). The results show that the leading plate speed is faster than trailing plate during the basin was extended between 50-26 Ma.

The drift rms velocity in the shaded area of model B (Fig. 16-B) which contains previous models (Yamazaki, 2010; Sdrolias et al., 2004) and our model illustrates that both leading and trailing plates were drifted by 14cm/yr. Although, spreading process had ceased.

The last model shown in figure 16-C is based on the global circuit plate reconstruction model (Seton et al., 2012) which contains previous magnetic isochrons (Hilde and Lee, 1984) for opening of the WPB. In the shaded area (Fig. 16-c), the rms speed of trailing plate exceeds that of the leading plate.

This study constrained that the half spreading rates of the basin is undergone in three main stages: 6.5cm/yr in 42-49 Ma, 4.0cm/yr in 37-42Ma, 0.5cm/yr in 37-26Ma (Fig. 17-A). Also, the opening direction over time variation was changed from NE-SW to N-S during 37-39Ma. There were short-term direction changes between 47-42Ma (Fig. 17-C)

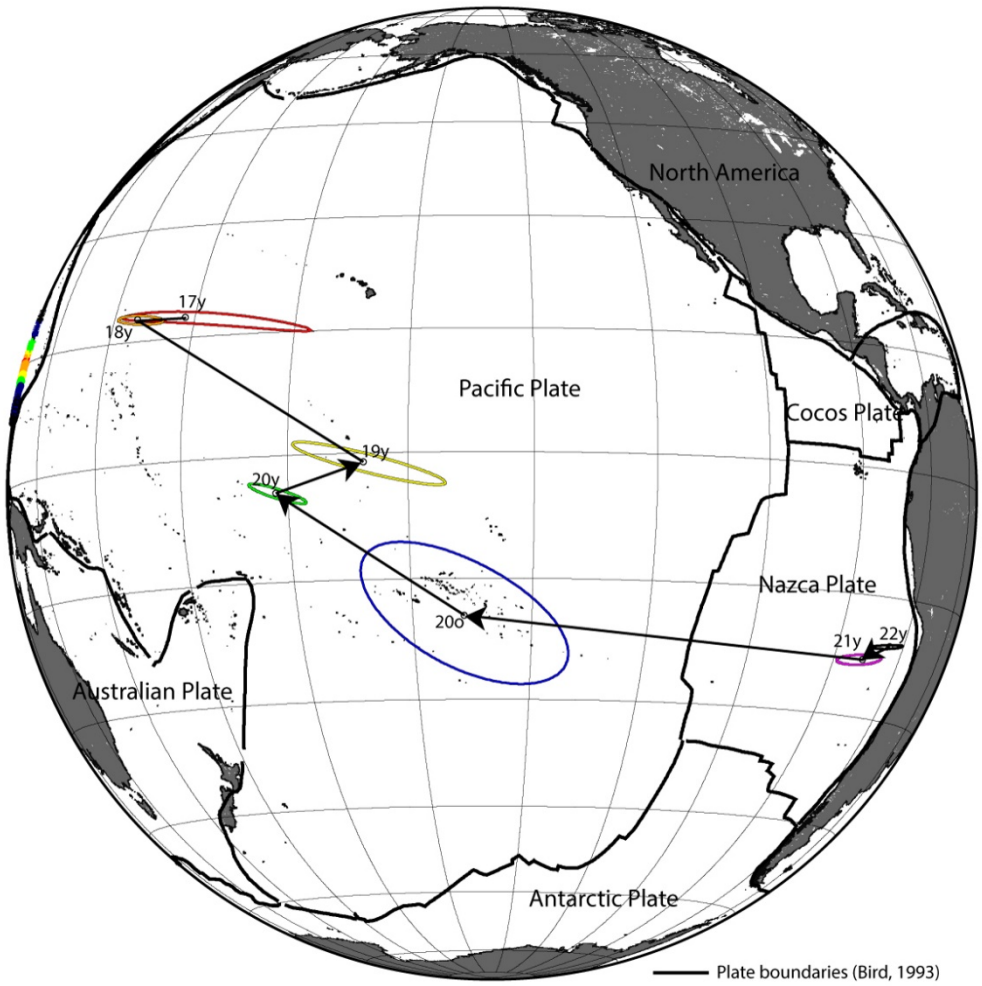

Figure 15. Finite rotation pole variation during extension in West Philippine Basin (chron 22y – 17y). Ellipses are 95% confidence limits. Thick black solid lines are plate boundaries (bird, 1993). Each finite rotation pole describes plate motions.

5. DISCUSSION

5.1 Characteristics of magnetic anomalies in the West Philippine Basin

In this study, various marine magnetic anomaly profiles and high-resolution bathymetry grid were examined to study the opening process of the WPB. We confirm that the observed vertical component magnetic anomalies accord with the 2-D synthetic vertical component model (Fig. 12). The comparison between vertical component magnetic anomaly and its synthetic model in the WPB indicates that the basin spreading took place during about 49 - 26Ma. Also we conclude that the basin underwent fast spreading process compared to the former study (Hilde and Lee, 1984).

In our study, we presume that the spreading from chron 17y to the CBR was slowly progressed. Because it is difficult to identify magnetic anomaly from the location of chron 17y to the CBR. Therefore, the age of dredge sample that Ar-Ar isotope analysis measures in the middle of the CBR from 28.10±0.16 Ma to 26.1±0.9 Ma (Fujioka et al., 1999) was reflected to our study.

The calculated MBSDs were likely to parallel with magnetic anomaly strikes on the basin. Directions of both strikes change from E-W to NNW-SSE in clock-wise far from the CBR (Fig. 14). However, a few MBSDs were observed not to match with the magnetic lineation strike and to display on the middle of the magnetic block (17.1 N, 132.8 E). This can be affected by radical topographic variations such as fracture zone (Seama et al., 1993).

The area (15˚N 128˚E-16˚N 129˚E) shown in Figure 14 seems to be a trapped tectonic block originated from north of the WPB. There are three evidences – 1. fracture zones, 2. negative free-air gravity anomalies, 3. Exceeding crustal accretion ratio. First, the bathymetry indicates that fracture zones were evolved along the boundary of the block. Second, the negative free-air gravity anomalies were displayed along the margin of the place. Third, the difference of crustal accretion between North and South in western side of the basin is large enough to support the existence of trapped block.

The magnetic anomalies in the SWPB near the West of the CBR were symmetric and weak negative. Whereas, the anomalies in conjugate region of NWPB were positive value. This means that complex extension process such as intermittent and extremely slow spreading (Deschamps et al., 2008) exists beside CBR between 26 to 36Ma. However, the evidences are not enough to corroborate the hypothesis because the data of magnetic anomaly and bathymetry in the area are still insufficient. So, this area needs more geophysical survey to understand in detail.

5.2 Kinematic reconstruction of the West Philippine Basin

The finite rotation poles which display kinematic motion of the plate (Cox and Hart, 1986) shifted to northward trend and approached to the CBR over time. This shift is due to the different plate rotation between leading and trailing plate.

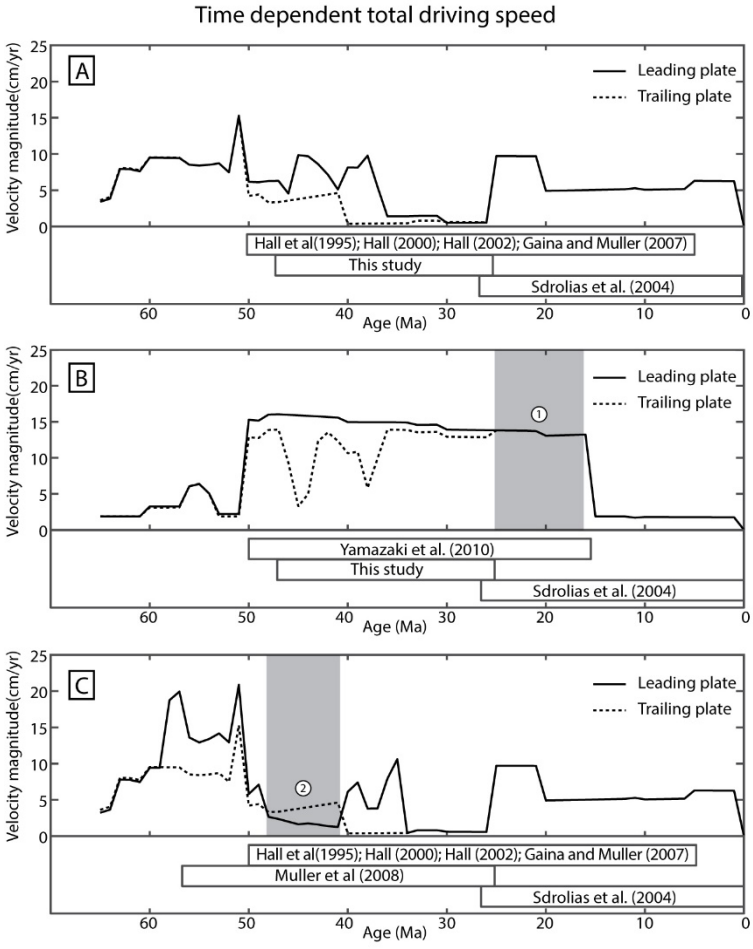

Figure 16. Time dependent absolute driving speed of each model. Model A consists of Paleo-magnetic model of Hall et al. 1995; Hall, 2000; Hall, 2002 and marine magnetic reconstruction model of this study. Model B is composed of paleo-magnetic model of Yamazaki et al. 2010 and marine magnetic reconstruction model of this study. Model C consists of Paleo-magnetic model by Hall et al. 1995; Hall, 2000; Hall, 2002. And marine magnetic reconstruction model by Hilde and Lee, 1984; Müller et al., 2008. All models contain the reconstruction model of Shikoku Basin and Parece-Vela Basin by marine magnetic isochrons of Sdrolias et al. 2004.

The NWPB, leading plate, was more actively rotated than that of SWPB. The finite rotation pole variations suggest that the opening of the WPB was not uniform and the motion transformation of NWPB was more significant than that of SWPB during the late stage of basin opening (present - 37Ma). This supports the idea of Okino and Fujioka (2003) that two different spreading processes occurred after chron 17y. This motion variation might have relation with the opening initiation of the Parece-Vela Basin caused by the subsidence of the Pacific Plate about 30Ma (e.g. Sdrolias et al., 2004).

The three different reconstruction models are compared by age dependent drift speed of the basin during its opening and shift. The drift speeds of the leading plate (NWPB) and trailing plate (SWPB) were calculated by rms method (Zahirovic et al., 2015) because the half spreading velocities were changed by the plate motion variations depending on each location of the plate.

Figure 16-A shows that the leading plate speed was faster than trailing plate when the basin was extended between 50-26 Ma. This result matches with previous study and supports the hypothesis that the plate came from south. The second model shown in figure 5-B indicates that the WPB was drifted by fast drifting speed about 14cm/yr without spreading process. However, there is little possibility for this model in natural condition when divergent boundary such as spreading ridge exists between two basins. The last model shown in figure16-C is based on the global circuit plate reconstruction (Seton et al., 2012) including Hilde and Lee (1984) for opening of the WPB. The trailing plate speed exceeding the leading plate speed in the shaded area (2) can be

explained by ridge subduction or extension process with fast rotation dominated by subduction pulling-force in the southern-most boundary. But, the WPB has been considered that it extended without ridge subduction, in addition, the subduction zones were developed in the Northern-most boundary of the basin compared to the southern-most boundary because the entire plate was shifted to the northward direction. Also spreading process from fast rotation of trailing plate cannot be explained by present tectonic configuration of the WPB. Hence, the first model is the most reliable among the three models.

The kinematic properties during the extension of the WPB were calculated from this study and previous model (Hilde and Lee, 1984). Usual measurement of half spreading rate in the plate is to compare magnetic anomaly with 2-D box forward model along the ship track which goes along the plate spreading direction. However, if the spreading direction was gradually varied or plate underwent rotation process or the ship track was not parallel to spreading direction, measuring half spreading rate is problematic. So, we computed the rms velocity of the WPB from finite rotation model based on magnetic anomaly analysis (Fig. 17).

This study indicates that the rms spreading velocity of the basin is continuously decreased during the opening (50–26 Ma). In addition, the rms half spreading rates can be constrained to three main phases: 6.5cm/yr in 42-49 Ma, 4.0cm/yr in 37-42Ma, 0.5cm/yr in 37-26Ma. These results provide that the opening speed of the WPB in early

stage was faster than the previous thought (c.f. 4.4 cm/yr in early stage and 1.8 cm/yr late stage).

The variation of spreading direction in WPB from previous marine magnetic studies (Deschamps and Lallemand, 2002; Taylor and Goodliffe, 2004; Hilde and Lee, 1984; Hall et al., 1995; Sasaki et al., 2014) maintains that spreading directions were changed from NW-SE to E-W in chron 20y (42 Ma). Also, the azimuth variation model from Hilde and Lee (1984) shows that the spreading directions were suddenly changed in 51Ma (Fig. 17-C). However, our model which combined with paleomagnetic studies (Hall et al. 1995; Hall, 2000; Hall, 2002) and marine magnetic study of Shikoku-Parece Vela Basin (Sdrolias et al., 2004) shown in figure 17-C indicates that there was significant spreading direction change between 39-37 Ma. This result slightly differs from the previous studies which the spreading directions were changed at least three times in 44Ma, 43Ma and 39Ma.

According to our analysis, the comparison between the change of spreading speed in each stage and its direction have no relationships. The south-west of the CBR and surrounded basin still remains lack of geophysical data to understand tectonic history of the Western Pacific. Therefore, additional geophysical survey should be required to solve the geodynamic puzzles in the tectonically complicated region.

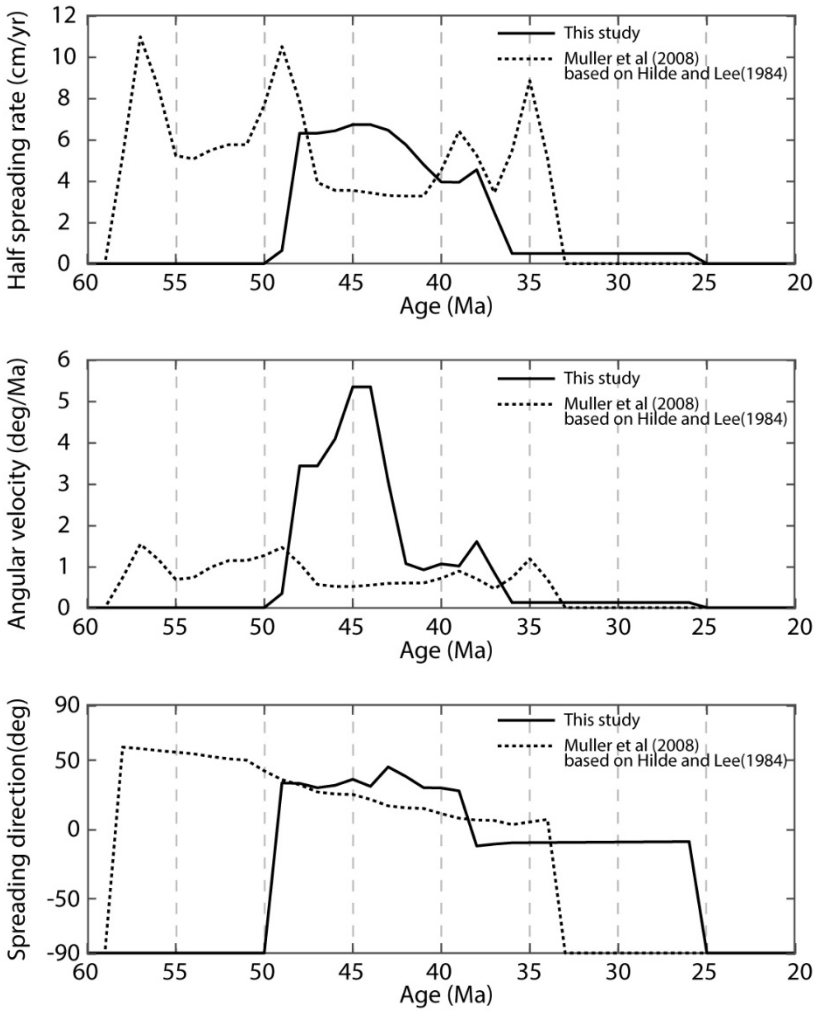

Figure 17. Kinematic properties during extension of the West Philippine Basin. The first graph (top) indicating half spreading rate variation over time. The second graph illustrating angular velocity over time and the third describing spreading direction changes over time. Solid line – this study, dotted line – Müller et al (2008) based on Hilde and Lee (1984).

6. CONCLUSION AND SUMMARY

We examined bathymetry and magnetic profiles to investigate the kinematic characteristics of the West Philippine Basin. Our study suggests the following conclusions.

Vertical component magnetic anomalies from STCM data are good method to determine magnetic isochrons compared to PPM data. Because the vertical vector anomaly does not affect by skewed horizontal field from spreading axis variation, the observed anomaly shows good connection with 2-D box anomaly model.

The identified magnetic lineation (Fig. 14) suggest that the spreading directions change gradually in anti-clock-wise direction from the ENE-WSW at older ages to N-S at the CBR. However, the combined stage pole model displays at least three different changes (Fig. 17-C).

Most of the seafloor fabric strikes in the West Philippine Basin have good correlations with MBSD. But, few MBSDs were not correlated with magnetic lineation strike and appeared on the radical topographic variation such as escarpment and fracture zone. Also, MBSDs in the north of Oki Daito Escarpment were not correlated with seafloor abyssal hill strikes in the area. Spreading direction and the spreading axis might not be perpendicular during the extension in early stage.

Spreading rate decreases from 6.5cm/yr to 4.5cm/yr and finally 0.5cm/yr before spreading cessation; these velocities are higher than those of 4.4cm/yr than 1.8cm/yr

proposed by a previous study (Watts et al., 1976; Mrozowski et al., 1982; Hilde and Lee, 1984; Okino et al., 2003; Deschamps and Lallemand, 2002)

Our results indicate that more spreading history would be exist in the south west of the CBR. However, in order to understand detailed motion of the WPB, additional survey should be required in the south-west of the CBR and surrounded basins.

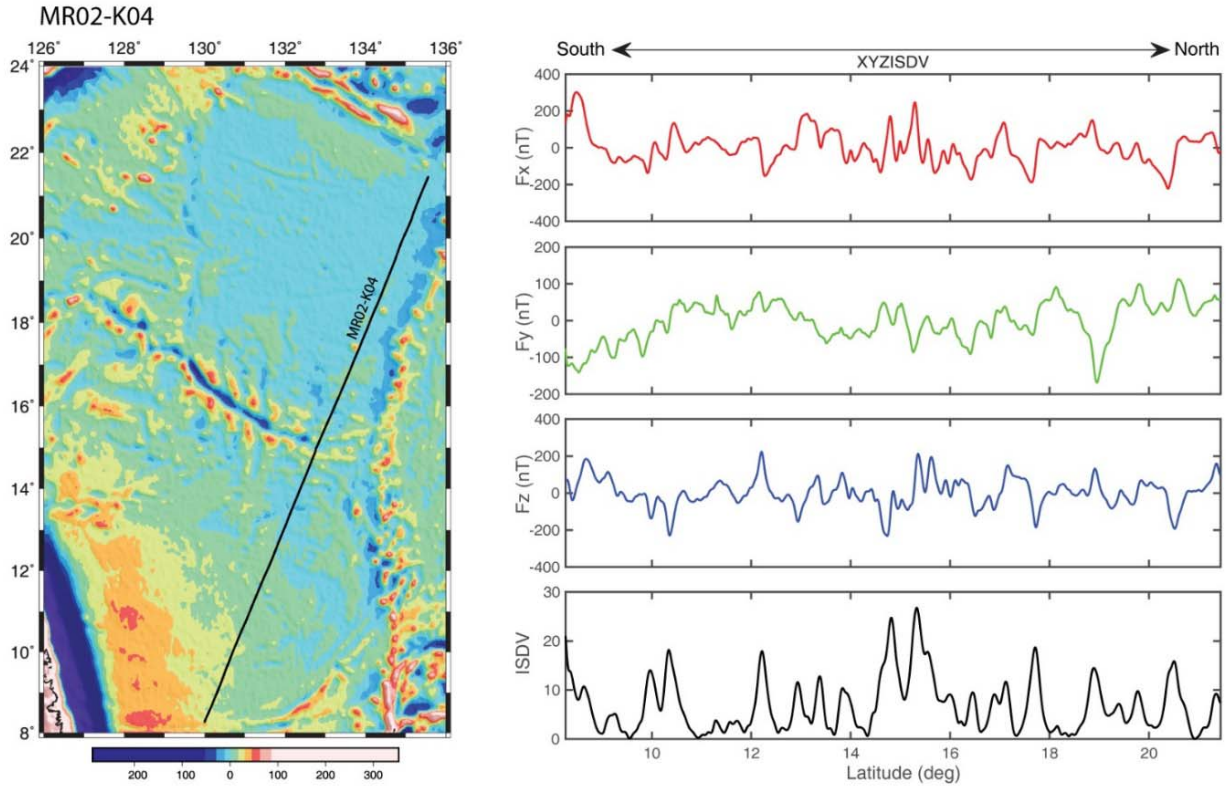

Figure 18. STCM survey track and three component magnetic anomalies with ISDV of the cruise MR02-K04 (line1).

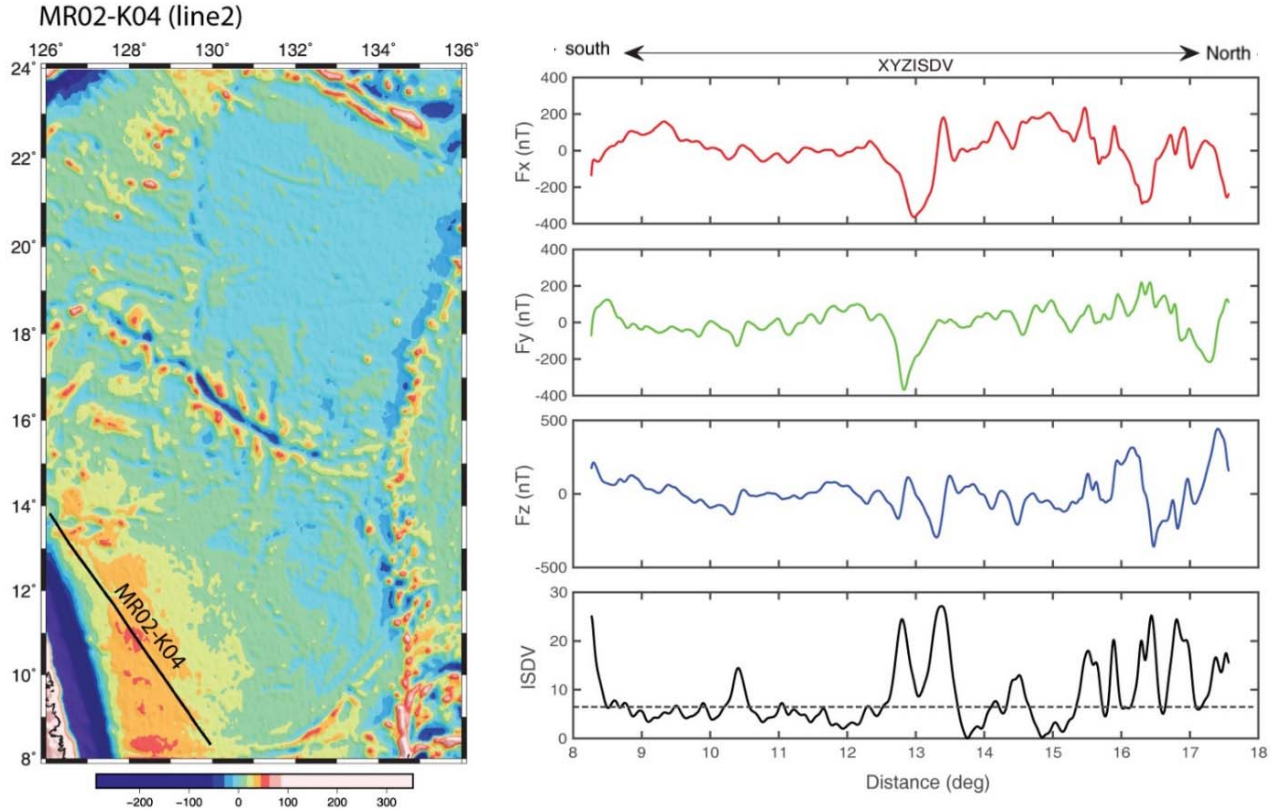

Figure 19. STCM survey track and three component magnetic anomalies with ISDV of the cruise MR02-K04 (line2).

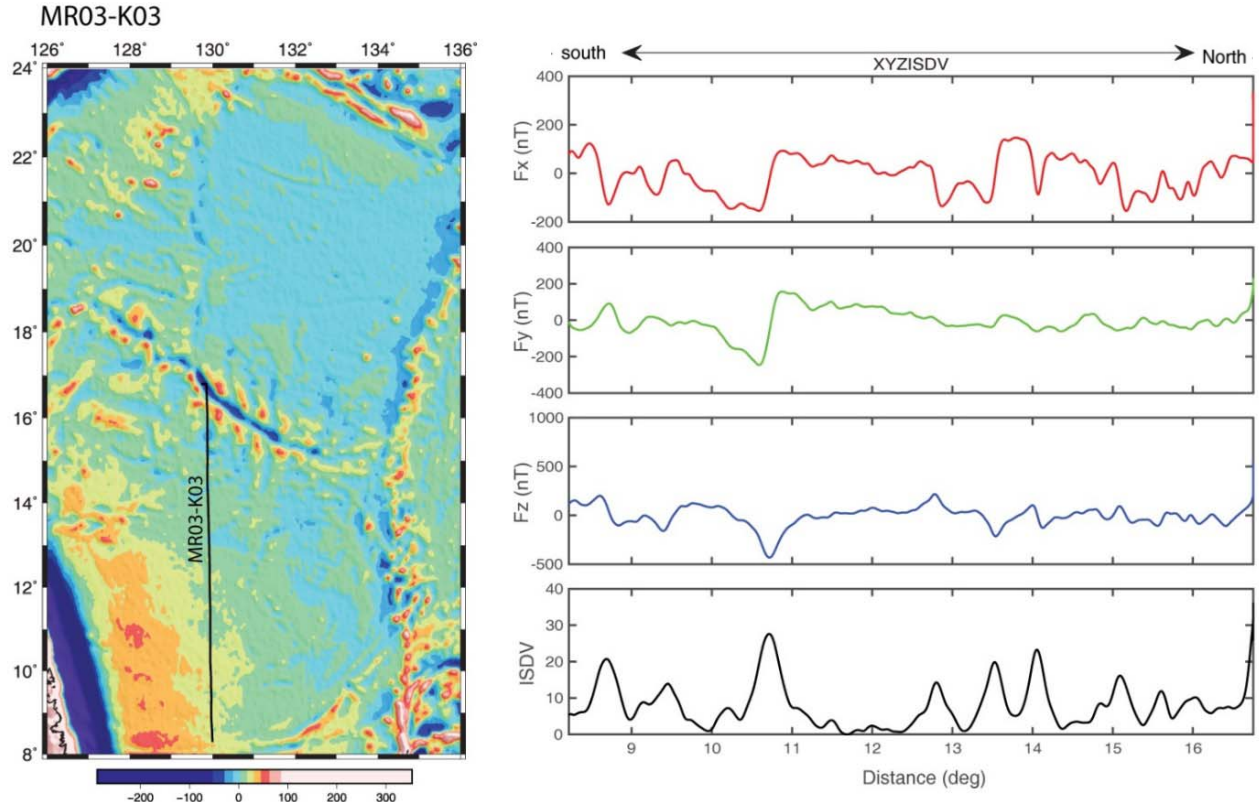

Figure 20. STCM survey track and three component magnetic anomalies with ISDV of the cruise MR03-K03.

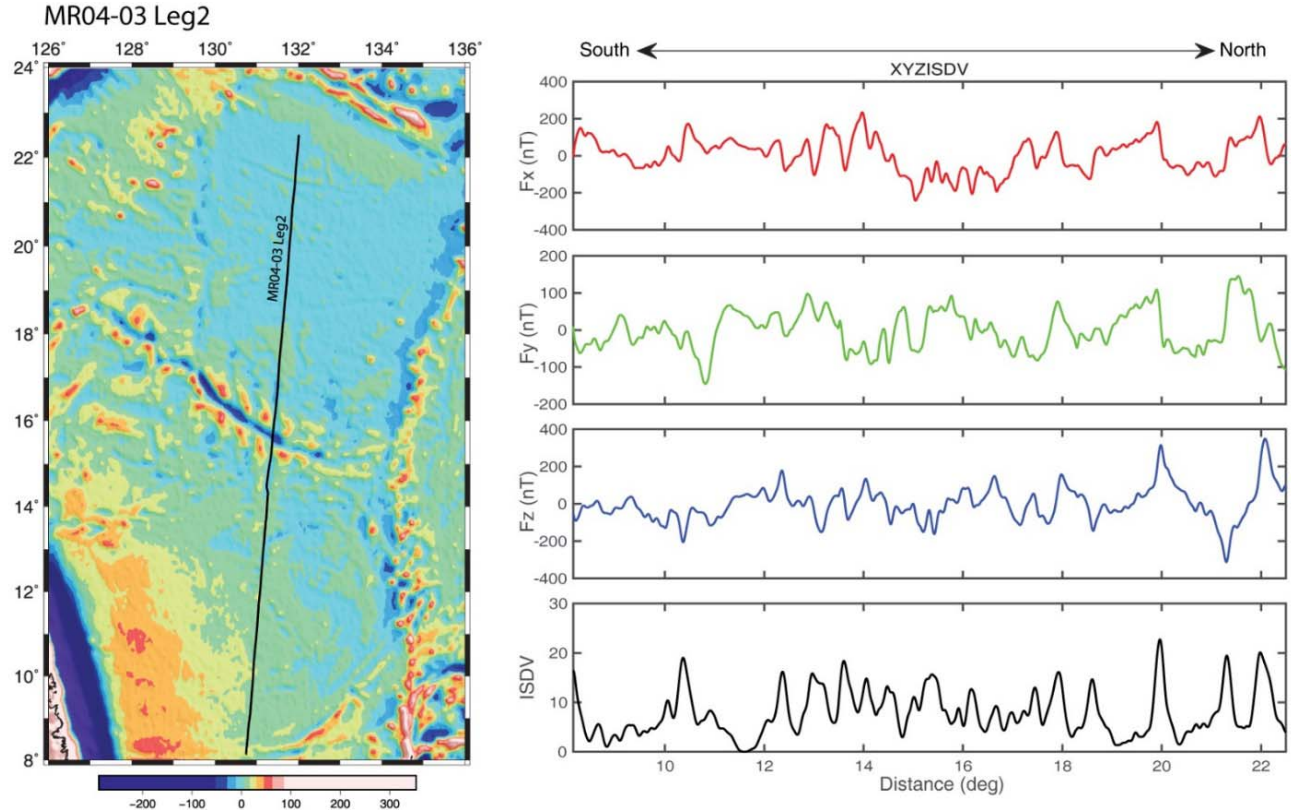

Figure 21. STCM survey track and three component magnetic anomalies with ISDV of the cruise MR04-03 Leg2.

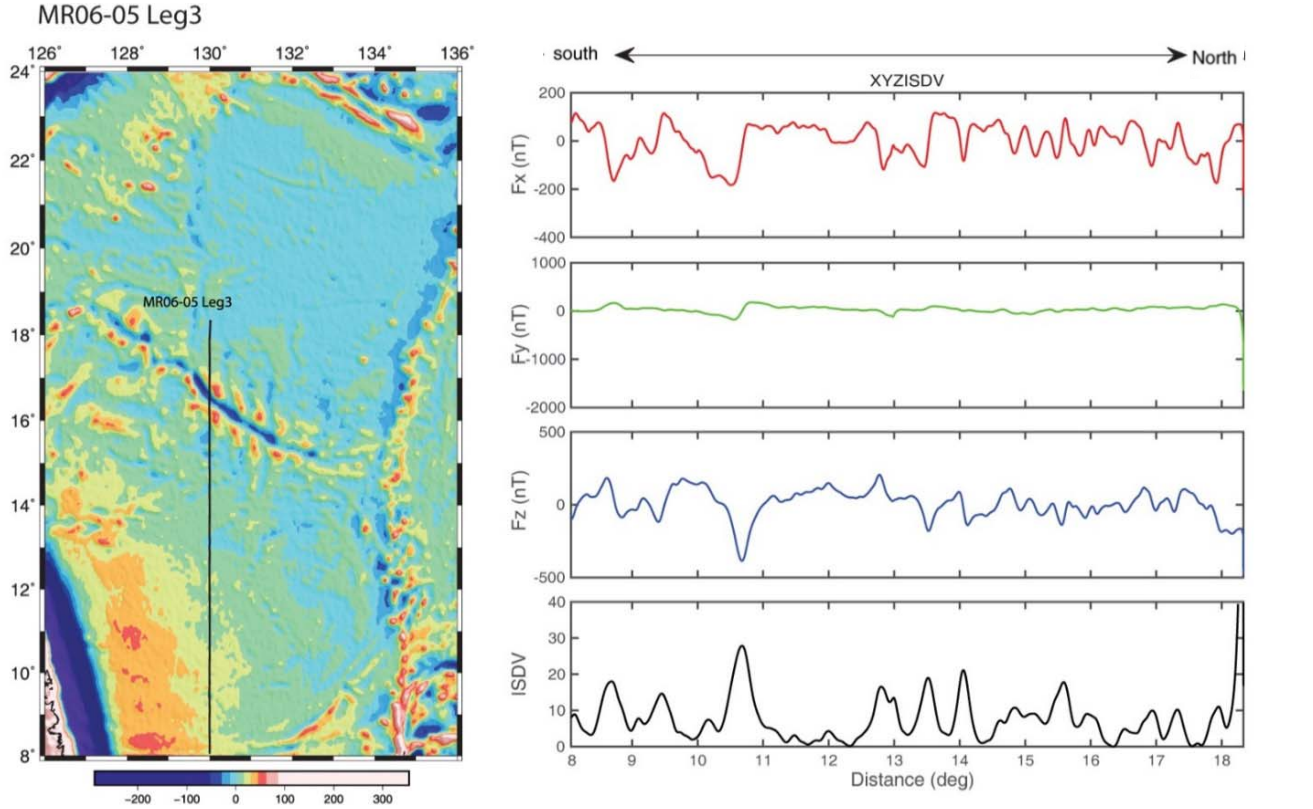

Figure 22. STCM survey track and three component magnetic anomalies with ISDV of the cruise MR06-05 Leg3.

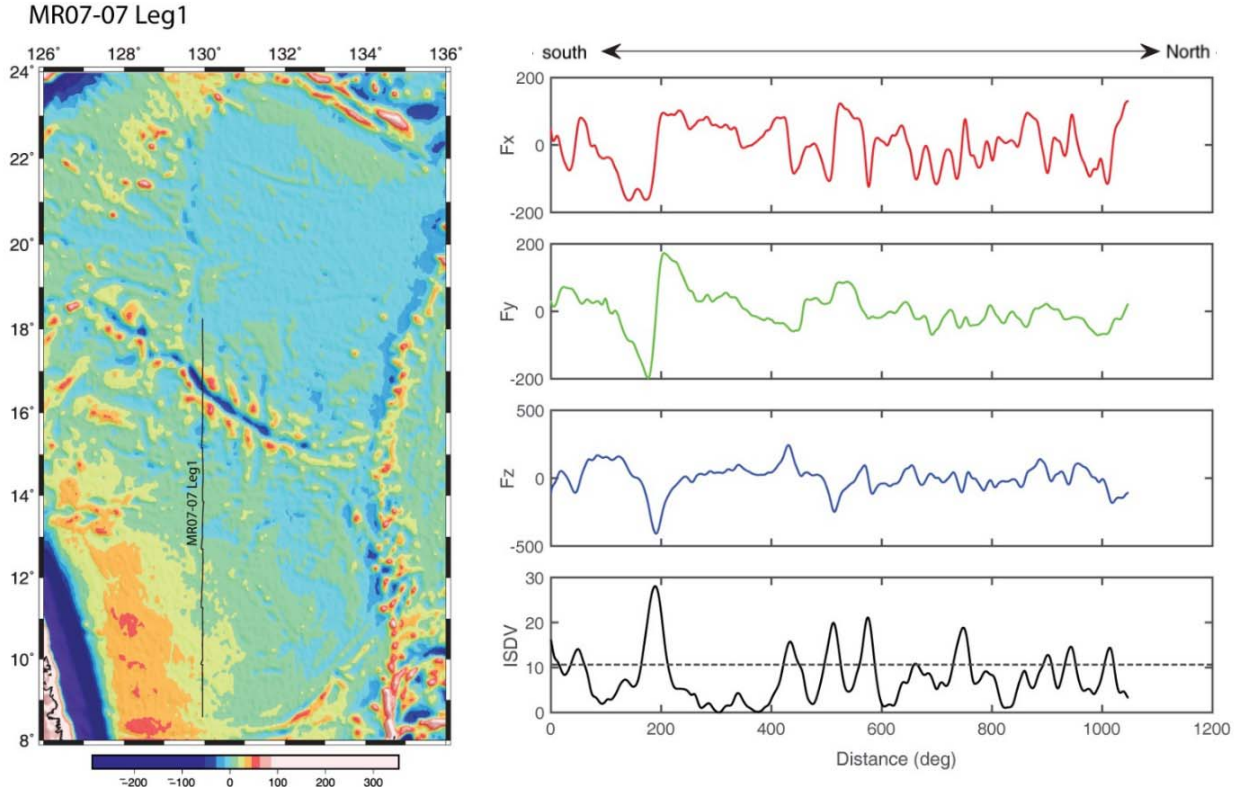

Figure 23. STCM survey track and three component magnetic anomalies with ISDV of the cruise MR07-07 Leg1.

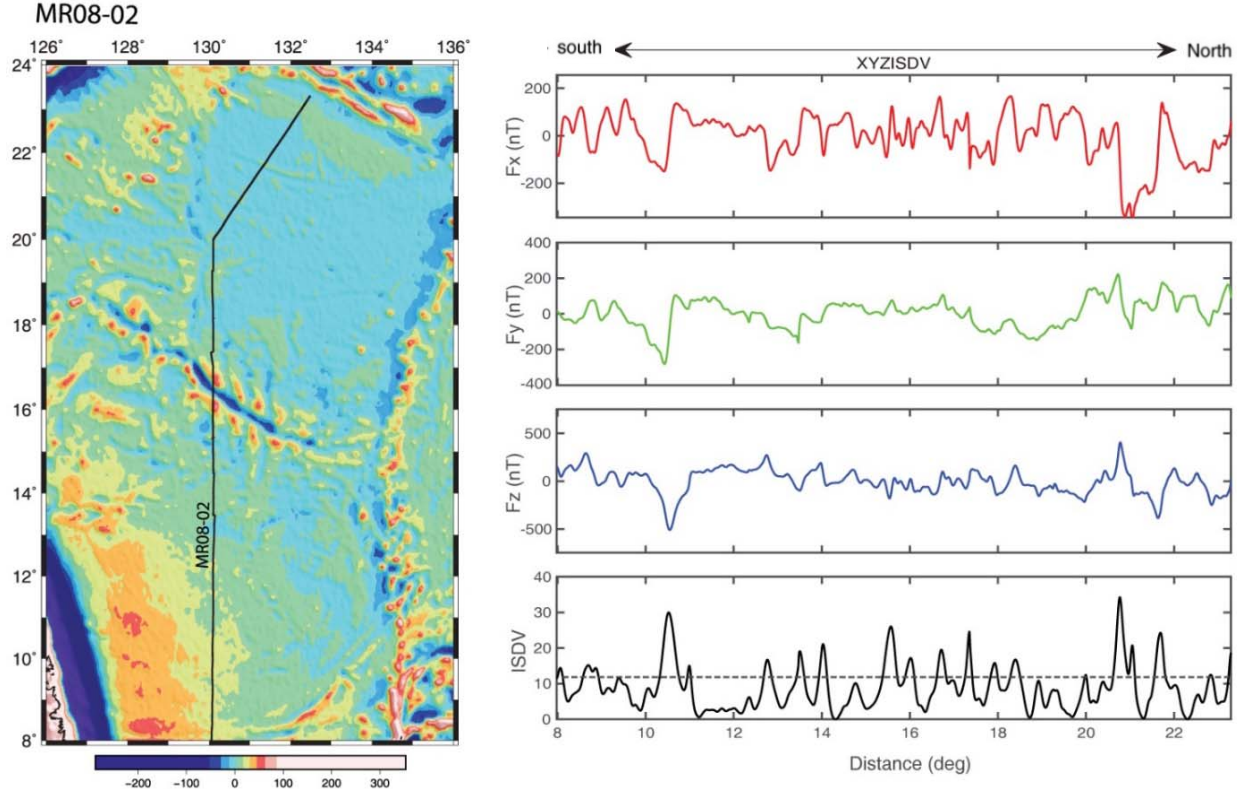

Figure 24. STCM survey track and three component magnetic anomalies with ISDV of the cruise MR08-02.

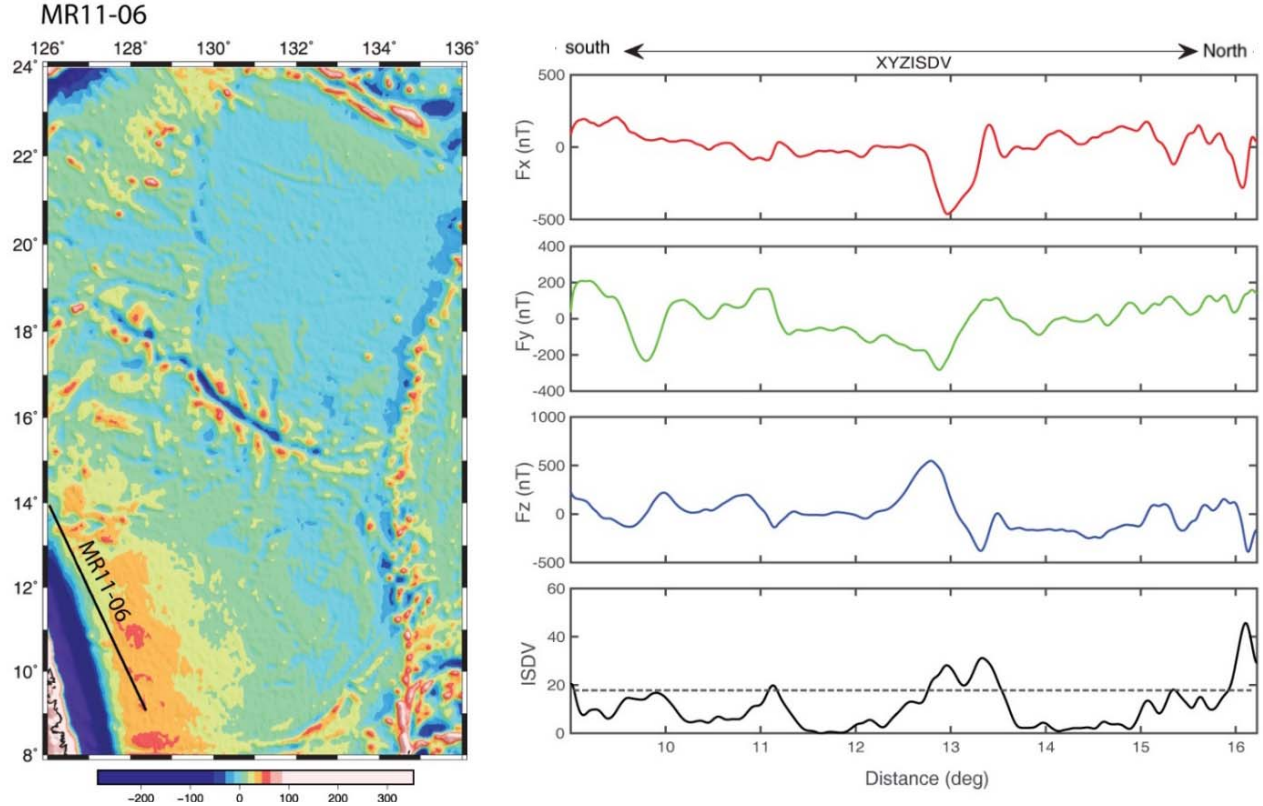

Figure 25. STCM survey track and three component magnetic anomalies with ISDV of the cruise MR11-06.

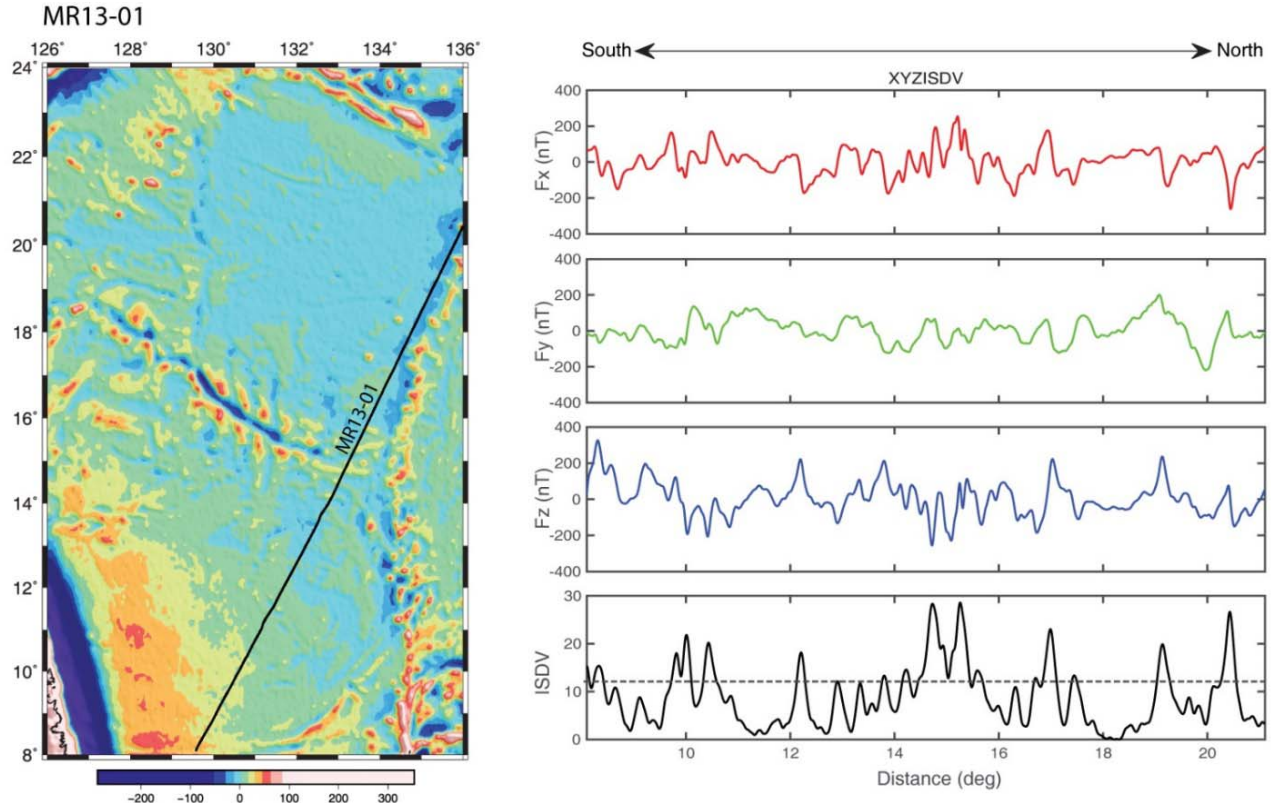

Figure 26. STCM survey track and three component magnetic anomalies with ISDV of the cruise MR13-01.

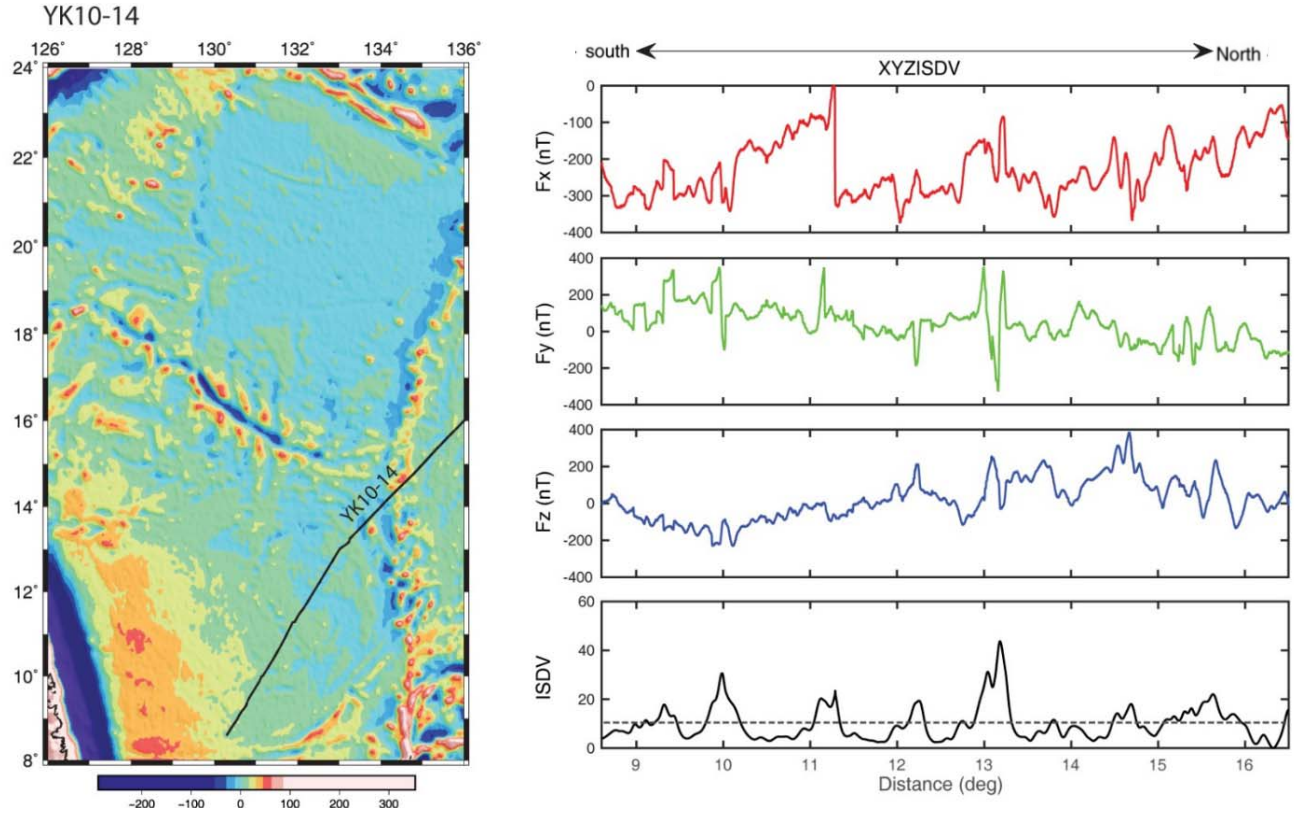

Figure 27. STCM survey track and three component magnetic anomalies with ISDV of the cruise YK10-14.

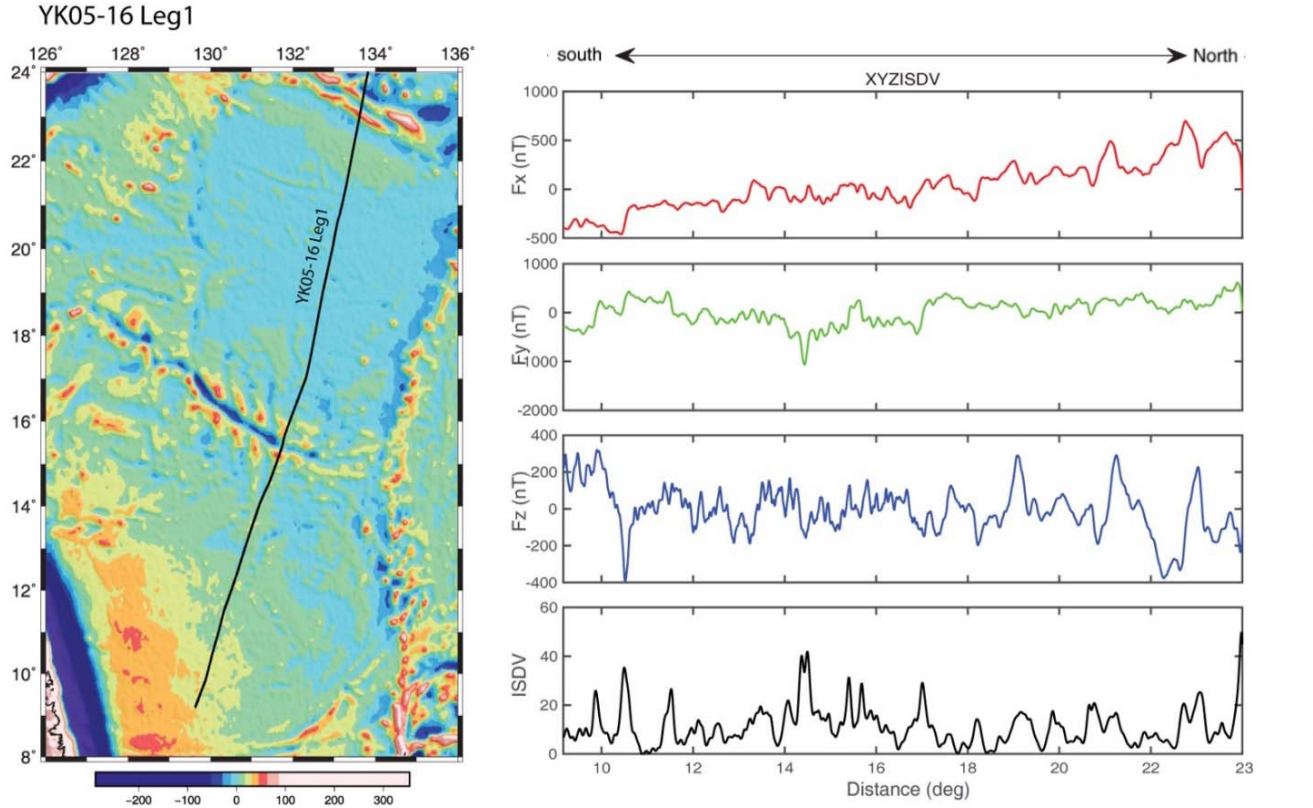

Figure 28. STCM survey track and three component magnetic anomalies with ISDV of the cruise YK05-16 Leg1.

REFERENCES

Andrews, J. E. (1980). Morphologic evidence for reorientation of sea-floor spreading in the West Philippine Basin. *Geology*, *8*(3), 140. http://doi.org/10.1130/0091-7613(1980)8<140:MEFROS>2.0.CO;2

Chang, T., Stock, J., Molnar, P., 1990. The rotation group in plate tectonics and the representation of uncertainties of plate reconstructions. Geophysical Journal International 101, 649–661.

Cox, A., Hart, R.B., 1986. Plate Tectonics: How It Works. Blackwell Scientific Publications, Oxford (382pp).

Dauteuil, O., & Brun, J.-P. (1996). Deformation partitioning in a slow spreading ridge undergoing oblique extension: Mohns Ridge, Norwegian Sea. *Tectonics*, *15*(4), 870–884. http://doi.org/10.1029/95TC03682

Dauteuil, O., Huchon, P., Quemeneur, F., & Souriot, T. (2001). Propagation of an oblique spreading centre: the western Gulf of Aden. *Tectonophysics*, *332*(4), 423–442. http://doi.org/10.1016/S0040-1951(00)00295-X

Dauteuil, O., & Brun, J.-P. (1993). Oblique rifting in a slow-spreading ridge. *Nature*, *361*(6408), 145–148. http://doi.org/10.1038/361145a0

Deschamps, A., & Lallemand, S. (2002). The West Philippine Basin: An Eocene to early Oligocene back arc basin opened between two opposed subduction zones. *Journal of Geophysical Research: Solid Earth*, *107*(B12), EPM 1–1–EPM 1–24. http://doi.org/10.1029/2001JB001706

Deschamps, A., Lallemand, S., & Dominguez, S. (1999). The last spreading episode of the West Philippine Basin revisited. *Geophysical Research Letters*, *26*(14), 2073–2076. http://doi.org/10.1029/1999GL900448

Deschamps, A., Shinjo, R., Matsumoto, T., Lee, C.-S., Lallemand, S. E., & Wu, S. (2008). Propagators and ridge jumps in a back-arc basin, the West Philippine Basin. *Terra Nova*, *20*(4), 327–332. http://doi.org/10.1111/j.1365-3121.2008.00824.x

Dilek, Y., & Furnes, H. (2014). Ophiolites and Their Origins. *Elements*, *10*(2), 93–100. http://doi.org/10.2113/gselements.10.2.93

Fujioka, K., Okino, K., Kanamatsu, T., Ohara, Y., Ishizuka, O., Haraguchi, S., & Ishii, T. (1999). Enigmatic extinct spreading center in the West Philippine backarc basin unveiled. *Geology*, *27*(12), 1135. http://doi.org/10.1130/0091-7613(1999)027<1135:EESCIT>2.3.CO;2

Goodman, D., & Bibee, L. D. (1989). Crustal Seismic Structure Beneath The West Philippine Sea, 17^{o} - 18^{o} North. *Marine Geophysical Researches*, *11*, 155–168.

Hall, R. (2002). Cenozoic geological and plate tectonic evolution of SE Asia and the SW Pacific. *Journal of Asian Earth Sciences*, *20*, 353–431.

Hall, R. (2000). Neogene history of collision in the Halmahera region, Indonesia, 27th Annual Convention Proceedings, 1-9

Hall, R., Fuller, M., Ali, J. R., & Anderson, C. D. (1995). The Philippine Sea Plate: Magnetism and reconstructions. In *Active Margins and Marginal Basins of the Western Pacific* (Vol. 88, pp. 371–404). http://doi.org/10.1029/GM088p0371

Hilde, W. C., & Lee, C.-S. (1984). ORIGIN AND EVOLUTION OF THE WEST PHILIPPINE BASIN: A NEW INTERPRETATION *. *Tectonophysics*, *102*, 85–104.

Hellinger, S.J., 1981. The uncertainties of finite rotations in plate tectonics. Journal of Geophysical Research 86, 9312–9318.

Horner-johnson, B. C., & Gordon, R. G. (2003). Equatorial Pacific magnetic anomalies identified from vector aeromagnetic data. *Geophysical Journal International*, *155*, 547–556.

Isezaki, N. (1986). A new shipboard three-component magnetometer. *GEOPHYSICS*, *51*(10), 1992–1998. http://doi.org/10.1190/1.1442054

Ishihara, T., & Koda, K. (2007). Variation of crustal thickness in the Philippine Sea deduced from three-dimensional gravity modeling. *Island Arc*, *16*(3), 322–337. http://doi.org/10.1111/j.1440-1738.2007.00593.x

Karig, D. E. (1962). 42. BASIN GENESIS IN THE PHILIPPINE SEA, 857–879.

Karig, D. E., Ingle, J. C., Bouma, A. H., Ellis, H., Haile, N. e. a., Koizumi, I., Ling, H. Y. (1973). Origin of the West Philippine Basin. *Nature*, *246*, 458–461.

König, M. (2005). Processing of shipborne magnetometer data and revision of the timing and geometry of the Mesozoic break-up of Gondwana. *Phd Thesis*, 139.

Korenaga, J. (1995). Comprehensive analysis of marine magnetic vector anomalies. *Journal of Geophysical Research: Solid Earth*, *100*(B1), 365–378. http://doi.org/10.1029/94JB02596

Lewis, S. D., and D. E. Hayes, The Tectonics of Northward Propagating Subduction Along Eastern Luzon, Philippine Islands, in The Tectonic and Geologic Evolution of South East Asian Seas and Islands, part 2, Geophys. Monogr. Ser., edited by D. E. Hayes, vol. 27, pp. 57 – 78, AGU, Washington, D. C., 1983.

Lewis, S. D., D. E. Hayes, and C. L. Mrozowski, The origin of the west Philippine basin by inter-arc spreading, Geology and tectonics of Luzon and Marianas region, in Proceedings of CCOP-IOC-SEATAR Workshop, Manila, Philippines, Spec.

Publ., edited by G. R. Blace and F. Zanoria, vol. 1, pp. 31 – 51, Philipp. SEATAR Comm., Manila, 1982.

Louden, K. E. (1980). The crustal and lithospheric thicknesses of the Philippine Sea as compared to the Pacific. *Earth and Planetary Science Letters*, *50*(1), 275–288. http://doi.org/10.1016/0012-821X(80)90138-7

Louden, K. E. (1976). *THE ORIGIN AND TECTONIC HISTORY OF THE SOUTH-WEST PHILIPPINE SEA*.

Mrozowski, C. L., Lewis, S. D., & Hayes, D. E. (1982). Complexities in the tectonic evolution of the West Philippine Basin. *Tectonophysics*, *82*(1-2), 1–24. http://doi.org/10.1016/0040-1951(82)90085-3

Müller, R. D., Sdrolias, M., Gaina, C., & Roest, W. R. (2008). Age, spreading rates, and spreading asymmetry of the world's ocean crust. *Geochemistry, Geophysics, Geosystems*, *9*(4), 1–19. http://doi.org/10.1029/2007GC001743

Müller, D., Gurnis, M., & Torsvik, T. (2011). GPlates Version 1.0. 1.

Nabighian, M. N. (1972). The Analytic Signal of Two-Dimensional Magnetic Bodies With Polygonal Cross-Section: Its Properties and Use for Automated Anomaly Interpretation. *Geophysics*, *37*(3), 507–517. http://doi.org/10.1190/1.1440276

Nishizawa, A., Kaneda, K., Katagiri, Y., & Oikawa, M. (2014). Wide-angle refraction experiments in the Daito Ridges region at the northwestern end of the Philippine Sea plate. *Earth, Planets and Space*, *66*(1), 25. http://doi.org/10.1186/1880-5981-66-25

Nogi, Y., & Kaminuma, K. (1999, November 25). Measurements of vector magnetic anomalies on board the icebreaker Shirase and the magnetization of the ship. *Annals of Geophysics*. http://doi.org/10.4401/ag-3711

Obayashi, M., Yoshimitsu, J., Nolet, G., Fukao, Y., Shiobara, H., Sugioka, H., Gao, Y. (2013). Finite frequency whole mantle P wave tomography: Improvement of subducted slab images. *Geophysical Research Letters*, *40*(21), 5652–5657. http://doi.org/10.1002/2013GL057401

Okino, K. (2003). The Central Basin Spreading Center in the Philippine Sea: Structure of an extinct spreading center and implications for marginal basin formation. *Journal of Geophysical Research*, *108*(B1), 1–18. http://doi.org/10.1029/2001JB001095

Okino, K., Ohara, Y., Kasuga, S., & Kato, Y. (1999). The Philippine Sea: New survey results reveal the structure and the history of the marginal basins. *Geophysical Research Letters*, *26*(15), 2287–2290.

Richter, C., & Ali, J. R. (2015). Philippine Sea Plate motion history : Eocene-Recent record from ODP Site 1201 , central West Philippine Basin. *Earth and Planetary Science Letters*, *410*, 165–173. http://doi.org/10.1016/j.epsl.2014.11.032

Royer, J.-Y., Chang, T., 1991. Evidence for relative motions between the Indian and Australian plates during the last 20Ma from plate tectonic reconstructions. Implications for the deformation of the Indo-Australian plate. Journal of Geophysical Research 89, 11,779–11,802.

Sasaki, T., Yamazaki, T., & Ishizuka, O. (2014). A revised spreading model of the West Philippine Basin. *Earth, Planets and Space*, *66*(1), 83. http://doi.org/10.1186/1880-5981-66-83

Schouten, H., & Cande, S. C. (1976). Palaeomagaetic Poles from Marine Magnetic Anomalies *. *Geophysical Journal of the Royal Astronomical Society*, *44*, 567–575.

Schouten, H., & McCamy, K. (1972). Filtering marine magnetic anomalies. *Journal of Geophysical Research*, *77*(35), 7089–7099. doi:10.1029/JB077i035p07089

Sdrolias, M., Roest, W. R., & Müller, R. D. (2004). An expression of Philippine Sea plate rotation: the Parece Vela and Shikoku Basins. *Tectonophysics*, *394*(1-2), 69–86. http://doi.org/10.1016/j.tecto.2004.07.061

Seama, N., Nogi, Y., & Isezaki, N. (1993). A New Method For Precise Determination of the Position and Strike of Magnetic Boundaries Using Vector Data of the Ge-

omagnetic Anomaly Field. *Geophysical Journal International*, *113*(1), 155–164. http://doi.org/10.1111/j.1365-246X.1993.tb02536.x

Seno, T., Stein, S., & Gripp, A. (1993). A Model for the Motion of the Philippine Sea Plate Consistent With NUVEL-1 and Geological Data. *Journal of Geophysical Research*, *98*(Figure 1), 17941–17948.

Seton, M., Müller, R. D., Zahirovic, S., Gaina, C., Torsvik, T., Shephard, G., … Chandler, M. (2012). Global continental and ocean basin reconstructions since 200Ma. *Earth-Science Reviews*, *113*(3-4), 212–270. http://doi.org/10.1016/j.earscirev.2012.03.002

Seton, M., Whittaker, J. M., Wessel, P., Müller, R. D., DeMets, C., Merkouriev, S., … Williams, S. E. (2014). Community infrastructure and repository for marine magnetic identifications. *Geochemistry, Geophysics, Geosystems*, *15*(4), 1629–1641. http://doi.org/10.1002/2013GC005176

Shih, T. C. (1980). Marine magnetic anomalies from the western Philippine Sea: implications for the evolution of marginal basins. *The Tectonic and Geologic Evolution of Southeast Asian Seas and Islands, Part. 1*, *23*, 49–75.

Spencer, S., Smith, D. K., Cann, J. R., Lin, J., & McAllister, E. (1997). Structure and stability of non-transform discontinuities on the Mid-Atlantic Ridge between 24^{o}N and 30^{o}N. *Marine Geophysical Researches*, *19*(4), 339–362.

Taylor, B., & Goodliffe, A. M. (2004). The West Philippine Basin and the initiation of subduction, revisited. *Geophysical Research Letters*, *31*(12), 2–5. http://doi.org/10.1029/2004GL020136

Uyeda, S., & Ben-Avraham, Z. (1972). Origin and development of the Philippine Sea. *Nature Phys Sci*, *240*, 176–178.

Watts, A. B., Weissel, J. K., & Larson, R. L. (1977). Sea-floor spreading in marginal basins of the Western Pacific. *Tectonophysics*, *37*(1-3), 167–181. http://doi.org/10.1016/0040-1951(77)90046-4

Yamazaki, T., Takahashi, M., Iryu, Y., Sato, T., Oda, M., Takayanagi, H., … Ooka, T. (2010). Philippine Sea Plate motion since the Eocene estimated from paleomagnetism of seafloor drill cores and gravity cores. *Earth, Planets and Space*, *62*(6), 495–502. http://doi.org/10.5047/eps.2010.04.001

Zahirovic, S., Müller, R. D., Seton, M., & Flament, N. (2015). Tectonic speed limits from plate kinematic reconstructions. *Earth and Planetary Science Letters*, *418*, 40–52. http://doi.org/10.1016/j.epsl.2015.02.037

요 약 문

필리핀판에 위치한 서필리핀 분지는 에오세 동안 빠른 확장을 겪은 것으로 생각된다. 하지만 지금까지의 판의 재구성 모델에서 이 분지의 자세한 확장과정과 주변 분지들과의 관계는 아직 논란의 여지가 되고있다. 그 이유는 (1) 한정된 해양 지자기 데이터 커버리지, (2) 분지의 복잡한 형성으로 인한 심한 지자기 왜곡 현상과 약한 자기이상대의 형성, (3) 판의 섭입으로 인해 분석의 어려움 등이 있다. 이 연구는 지난 수십년동안 축적된 해양지자기와 다중빔음향측심 데이터를 이용하여 판의 확장에 대하여 다시 연구를 하였다. 선상 삼성분자력계는 탐사가 용이하고 수직자력벡터만 측정이 가능하여 수평자력이상의 왜곡현상을 받지 않아 해석 또한 매우 용이하다. 하지만 배의 자세와 그것의 자화에 의한 노이즈를 제거하는 데이터 프로세스는 매우 복잡하다. 따라서 삼성분 자력 데이터의 신뢰성을 확보하기 위해 위 데이터로 계산된 자기경계주향도표 (MBSD)를 심해 구릉의 주향과 자력연대곡선과 비교해본 결과, 상호간의 상당한 일치성을 확인할 수 있었고 지자기 연대는 22y (49 Ma)까지 확인할 수 있었다. 하지만 분지의 일부가 섭입되어 지자기를 모델과 비교할 수 없기 때문에 남쪽의 일부분지에서의 오래된 지자기이상대를 결정할 수 없었다. 이러한 신뢰도를 바탕으로 각각의 지자기

연대에서 보다 자세한 오일러 유한회전극을 G-plates 프로그램을 이용하여 계산한 결과 서필리핀분지는 지자기 연대 22y (49 Ma)에서 동북동-서남서 방향으로 확장을 시작했고 지자기 연대 21y (45Ma)부터 남-북 방향으로 점차 확장 방향이 바뀌었다. 판의 시간 별 rms속도를 측정한 결과 기존에 보고된 판의 속도보다 짧은 기간 동안 빠른 확장이 일어난 것으로 나타났다. 분지의 확장은 37Ma에 확장 속도가 급격히 줄어 26Ma에 멈춘 것으로 사료된다. 우리의 분석에 따르면 서필리핀분지의 북쪽과 남쪽의 불균형 확장은 확장이 끝나갈수록 점점 더 커지는 것으로 관측되었다. 해양자기이상대 분석은 만약 분지 또는 판의 일부가 섭입을 했거나 복잡한 형성과정을 거쳤을 경우 분석이 매우 제한적일 수 있다. 하지만 해양 지자기 데이터는 측정 지역의 대표적인 지자기 방향을 나타내기 때문에 축적된 데이터 판의 운동학적 모델의 재구성에는 중요한 요소로 작용될 수 있다.

주요어: 서필리핀분지, 오일러극, 자기이상대, 지자기 연대, 판 재구성

학번: 2012-23083